



UNIVERSITÀ
DEGLI STUDI
FIRENZE

FLORE

Repository istituzionale dell'Università degli Studi di Firenze

Comparison of chemometric strategies for potential exposure marker discovery and false-positive reduction in untargeted metabolomics:

Questa è la versione Preprint (Submitted version) della seguente pubblicazione:

Original Citation:

Comparison of chemometric strategies for potential exposure marker discovery and false-positive reduction in untargeted metabolomics: application to the serum analysis by LC-HRMS after intake of Vaccinium fruit supplements / Renai L.; Ancillotti C.; Ulaszewska M.; Garcia-Aloy M.; Mattivi F.; Bartoletti R.; Del Bubba M.. - In: ANALYTICAL AND BIOANALYTICAL CHEMISTRY. - ISSN 1618-2642. - STAMPA. - 414:

Availability:

The webpage <https://hdl.handle.net/2158/1256644> of the repository was last updated on 2022-02-16T22:54:44Z

Published version:

DOI: 10.1007/s00216-021-03815-5

Terms of use:

Open Access

La pubblicazione è resa disponibile sotto le norme e i termini della licenza di deposito, secondo quanto stabilito dalla Policy per l'accesso aperto dell'Università degli Studi di Firenze (<https://www.sba.unifi.it/upload/policy-oa-2016-1.pdf>)

Publisher copyright claim:

La data sopra indicata si riferisce all'ultimo aggiornamento della scheda del Repository FloRe - The above-mentioned date refers to the last update of the record in the Institutional Repository FloRe

(Article begins on next page)



Comparison of chemometrics workflows for potential exposure markers discovery and false positive reduction in untargeted metabolomics: application to the serum analysis by LC-HRMS after intake of Vaccinium fruits supplements

Journal:	<i>Analytical and Bioanalytical Chemistry</i>
Manuscript ID	Draft
Type of Paper:	Research Paper
Date Submitted by the Author:	n/a
Complete List of Authors:	Renai, Lapo; UNIVERSITY OF FLORENCE, DEPARTMENT OF CHEMISTRY Ancillotti, Claudia; UNIVERSITY OF FLORENCE, DEPARTMENT OF CHEMISTRY Ulaszewska, Marynka ; IRCCS Ospedale San Raffaele, Center for Omics Sciences, Proteomics and Metabolomics Facility (ProMeFa) Garcia-Aloy, Mar; Edmund Mach Foundation Research and Innovation Centre, Metabolomics Unit, Department of Food Quality and Nutrition Mattivi, Fulvio; University of Trento Department of Cellular Computational and Integrative Biology Bartoletti, Riccardo; University of Pisa, Department of Translational Research and New Technologies DEL BUBBA, MASSIMO; UNIVERSITY OF FLORENCE, DEPARTMENT OF CHEMISTRY
Keywords:	untargeted metabolomics, multivariate analysis, univariate parametric analysis, univariate non-parametric analysis, exposure markers, nutrikINETIC



UNIVERSITÀ
DEGLI STUDI
FIRENZE

DIPARTIMENTO
DI CHIMICA
"UGO SCHIFF"

EDITORIAL OFFICE
Analytical and Bioanalytical Chemistry

Dear Editor,

I send you the manuscript entitled "Comparison of chemometrics workflows for potential exposure markers discovery and false positive reduction in untargeted metabolomics: application to the serum analysis by LC-HRMS after intake of *Vaccinium* fruits supplements" for the submission to Analytical and Bioanalytical Chemistry.

Corresponding author and the submitter of the manuscript: Prof. Massimo Del Bubba, Department of Chemistry, University of Florence, Via della Lastruccia n.3, 50019 Sesto Fiorentino (Florence), Italy. E-mail address: massimo.delbubba@unifi.it

In this paper, we performed a non-trivial comparison of different chemometrics workflows for potential exposure markers (PEMs) discovery in nutrimetabolomics, identifying a novel chemometrics strategy that allows for reducing the false discovery selection of features, which were conversely retained in the highly populated group of "significant features", generated by other statistical methods, commonly adopted in literature.

An untargeted LC-HRMS study of serum samples from interventions with *Vaccinium myrtillus* (VM) and *Vaccinium corymbosum* (VC) supplements was chosen as representative in the field of LC-HRMS nutrimetabolomics, since it results in very complex outputs of data, which require the implementation of proper chemometrics workflows for data pretreatment and PEMs selection.

This aspect is often disregarded in metabolomics studies, where only one chemometrics protocol is applied without any explanation and in some cases protocols for PEMs discovery are even used not properly, e.g. when univariate

Prof. Massimo Del Bubba

Via della Lastruccia, 3 – 50019 Sesto Fiorentino (Firenze)
phone +39 055 4573326 | e-mail: massimo.delbubba@unifi.it
P.IVA | Cod. Fis. 01279680480



parametric tests are used without verifying normality and homoscedasticity of data distributions or in absence of these prerequisites.

Twelve PEMs related to the intake of bilberry and/or blueberry supplements were annotated in serum samples, five of them (i.e. octahydro-methyl- β -carboline-dicarboxylic acid and tetrahydro-methyl- β -carboline-dicarboxylic acid for VC, citric acid for VM, and caprylic acid and azelaic acid for both VC and VM) reported here for the first time as serum metabolites of these interventions, thus representing an additional element of novelty.

The comparison of the two interventions through a rigorous chemometrics approach, based on the analysis of the area under the curve of the longitudinal dataset followed by principal component analysis and linear discriminant analysis, highlighted thirteen statistically significant PEMs discriminating the two interventions, including four intra-intervention relevant metabolites (i.e. abscisic acid glucuronide, catechol sulphate, methyl-catechol sulphate, and α -hydroxy-hippuric acid). All these findings represent a further novelty element.

Based on the "Aims and Scope" of Analytical and Bioanalytical Chemistry, encouraging the publication of papers dealing with advanced chemometrics data analysis and omics analytical strategies, and the manuscript contents, I think that this paper is in line with the scope of Analytical and Bioanalytical Chemistry and it has enough quality to deserve the publication in this high reputable journal.

I thank you in advance for your consideration and I send you my best regards.

Sesto Fiorentino, October, 5th 2021

Massimo Del Bubba

A handwritten signature in black ink, reading 'Massimo Del Bubba', is shown within a light gray rectangular box.

1
2
3
4
5
6
7
8
9
10
11
12
13
14
15
16
17
18
19
20
21
22
23
24
25
26
27
28
29
30
31
32
33
34
35
36
37
38
39
40
41
42
43
44
45
46
47
48
49
50
51
52
53
54
55
56
57
58
59
60



Comparison of chemometrics workflows for potential exposure markers discovery and false positive reduction in untargeted metabolomics: application to the serum analysis by LC-HRMS after intake of *Vaccinium* fruits supplements

Lapo Renai^a, Claudia Ancillotti^a, Marynka Ulaszewska^{b,c}, Mar Garcia-Aloy^c, Fulvio Mattivi^d,
Riccardo Bartoletti^e, Massimo Del Bubba^{a*}

a) Department of Chemistry, University of Florence, Via della Lastruccia 3, 50019 Sesto Fiorentino (Florence, Italy)

b) IRCCS Ospedale San Raffaele, Center for Omics Sciences, Proteomics and Metabolomics Facility (ProMeFa), Via Olgettina, 60, 20132 Milan (Italy)

c) Metabolomics Unit, Department of Food Quality and Nutrition, Research and Innovation Centre, Fondazione Edmund Mach (FEM), Via Mach 1, 38098 San Michele all'Adige (Trento, Italy)

d) Department of Cellular, Computational, and Integrative Biology (CIBIO), University of Trento, Via Sommarive 9, 38123 Povo (Trento, Italy)

e) Department of Translational Research and New Technologies, University of Pisa, Via Risorgimento 36, 56126 Pisa (Italy)

* Corresponding author – phone number: +39 055 4573326; e-mail address: massimo.delbubba@unifi.it

Abstract

Untargeted liquid chromatographic-high resolution mass spectrometric (LC-HRMS) metabolomics for potential exposure markers (PEMs) discovery in nutrkinetic studies generates complex outputs. The correct selection of statistically significant PEMs is a crucial analytical step for understanding nutrition-health interactions. Hence, in this paper different chemometrics selection workflows for PEMs discovery, using multivariate or univariate parametric or non-parametric data analyses were comparatively tested and evaluated. The PEMs selection protocols were applied to a small sample size untargeted LC-HRMS study of a longitudinal set of serum samples from 20 volunteers after a single intake of (poly)phenolic-rich *Vaccinium myrtillus* and *Vaccinium corymbosum* supplements. The non-parametric Games-Howell test identified a restricted group of significant features, thus minimizing the risk of false positive retention. Among the forty-seven PEMs exhibiting a statistically significant postprandial kinetics, twelve were successfully annotated as purine pathway metabolites, benzoic and benzodiol metabolites, indole alkaloids, and organic and fatty acids, and five (i.e. octahydro-methyl- β -carboline-dicarboxylic acid, tetrahydro-methyl- β -carboline-dicarboxylic acid, citric acid, caprylic acid, and azelaic acid) were associated to *Vaccinium* berry consumption for the first time. The analysis of the area under the curve of the longitudinal dataset highlighted thirteen statistically significant PEMs discriminating the two interventions, including four intra-intervention relevant metabolites (i.e. abscisic acid glucuronide, catechol sulphate, methyl-catechol sulphate, and α -hydroxy-hippuric acid). Principal component analysis and samples classification through linear discriminant analysis performed on PEMs maximum intensity confirmed the discriminating role of these PEMs.

Keywords: untargeted metabolomics; multivariate analysis; univariate parametric analysis; univariate non-parametric analysis; exposure markers; nutrkinetic

1 Introduction

Untargeted metabolomics has been extensively recognized as the leading approach for the investigation of potential exposure markers (PEMs) of food (1, 2), also in relation to food-health interaction studies (3) (i.e. nutrimetabolomics), as it allows in principle the comprehensive overview of the human metabolome. Untargeted metabolomics platforms usually consist in liquid chromatography (LC) hyphenated with high-resolution mass spectrometry (HRMS), which guarantees the determination of a much larger number of biological metabolites and/or a more comprehensive structural investigation, compared to other techniques such as gas chromatography coupled to HRMS or LC coupled to nuclear magnetic resonance (4).

The use of LC-HRMS platforms in nutrimetabolomics generally results in very complex outputs of data, which require the implementation of proper workflows for their pretreatment and processing (5). Currently, no standard protocol has been defined to this aim, even though many workflows of data processing and analysis have been proposed (6). Data handling is usually performed by chemometrics tools, specifically selected according to the study design adopted, which may largely vary depending on a number of factors, such as study design (i.e. cross over or parallel), the number of interventions, sample size, and data acquisition strategies (e.g. standalone full scan or coupled with MSⁿ acquisitions) (5, 7). In nutrimetabolomics studies, food PEMs discovery commonly involves the application of multivariate analysis, using partial least square-discriminant analysis (PLS-DA) and the variable importance in projection (VIP) classifier as filtering strategy of statistically significant features from the original dataset (8-10). However, multivariate methods such as PLS-DA-VIP, due to their probabilistic nature, tend to select false positive (variables not causally related to groups) and/or false negative (missing of relevant features) (11). On the other hand, the multiple univariate approaches, which have been applied less frequently in nutrimetabolomics, although

not associated *per se* with false discovery risks, need the verification of some data distribution pre-requisites, i.e. normality or homoscedasticity (12). However, it should be emphasized that multiple univariate approaches have been frequently applied as parametric methods (e.g. *t*-test and ANOVA), although the sample size was so small to suggest the absence of the aforementioned prerequisite (13, 14), thus involving a high risk of generating false positive. In order to reduce the false positive risk, an adjustment of the false positive rate should be performed for the application of multiple inference tests (15). Conversely, the use of non-parametric tests is much less investigated (16), although the application of this type of chemometrics tools would release the data analysis procedure from the constraints of homoscedasticity and normal distribution of data.

Even though the impact of different chemometrics tools in the PEMs selection is expected to be remarkable, this issue is poorly investigated in the literature, especially in LC-HRMS nutrimental studies that, as mentioned before, are prone by their nature to generate a large number of features to be tested for their statistical significance (17). It is therefore important to compare the effects of the use of different chemometrics approaches for the selection of statistically significant PEMs. This issue is particularly important in the light of the intrinsic complexity of the biological fluids (e.g. serum and urine) investigated in this type of studies. Among these matrices, serum and plasma are particularly relevant as matrices that contain substances responsible for a direct biological activity, the study of which is of remarkable importance to establish a cause-effect role between the intake of a certain food and the human health benefits.

Based on the aforementioned considerations, this paper aimed at comparing the effectiveness of chemometrics protocols for PEMs discovery and false positive reduction, using different data analysis approaches, which included the widely adopted PLS-DA-VIP, the parametric *t*-test (before and after *P*-value adjustment), and the non-parametric Wilcoxon and Games-

101 Howell tests (*P*-value adjusted for both tests), the latter never investigated before in untargeted
102 nutrimentalomics.

103 The protocols have been tested on the untargeted LC-HRMS analysis of serum samples from
104 an intervention study of *Vaccinium myrtillus* (VM) and *Vaccinium corymbosum* (VC)
105 supplements as a representative application. In this regard, it should be emphasized that this
106 kind of application is of considerable intrinsic importance for nutrimentalomics purposes. In
107 fact, among fruits, small berries represent an abundant source of phenolic compounds in human
108 diet (18). In detail, the fruits belonging to the *Vaccinium* genus, above all *V. myrtillus* berries,
109 have been suggested as functional foods and used for supplement and drug preparation (19,
110 20). Moreover, *in vitro* studies have shown anti-proliferative and pro-apoptotic effects of
111 polyphenol-rich berry extracts against different prostate cancer cell lines (21) and the
112 chemopreventive properties of an anthocyanin-rich *V. myrtillus* extract were suggested in a
113 pilot study with patients affected by colon cancer (22). It should also be noted that few targeted
114 (23, 24) and only one untargeted (1) metabolomics studies have been published so far on human
115 serum and urinary (poly)phenolic metabolites of *Vaccinium* berries. **Figure 1** illustrates a
116 comprehensive and intuitive scheme of the analytical workflow adopted in this study for the
117 PEMs discovery in human serum after the administration of bilberry or blueberry supplement.

118 2 Material and Methods

119 2.1 Reagents and standards

120 Methanol and acetonitrile LC-MS Ultra CHROMASOLV™ and formic acid were purchased
121 from Sigma Aldrich (St. Louis, MO, USA). The ultrapure water was obtained by purifying
122 demineralized water in a Milli-Q system from Millipore (Bedford, MA, USA). O-hydroxy-
123 hippuric acid, abscisic acid, azelaic acid, 1-methyl-1,2,3,4-tetrahydro-β-carboline-3-carboxylic
124 and L-tryptophan-2',4',5',6',7'-d5 (TRI-d5) reference standards were obtained from Sigma

125 Aldrich, while trans-cinnamic-d5 acid (CIN-d5), N-Benzoyl-d5-glycine (Hippuric acid-d5,
126 HIP-d5) from CDN ISOTOPES Inc.

127 2.2 *Vaccinium myrtillus* and *Vaccinium corymbosum* berry supplements

128 The supplements were obtained by cryo-milling VM and VC freeze-dried berries, as detailed
129 in the section 1 of the *Supplementary material*. The supplements were characterized for total
130 soluble polyphenols, total monomeric anthocyanins and for some phenolic compounds, using
131 methods elsewhere described (25). Full details of the characterization analysis (**Tables S1 and**
132 **S2**) and results obtained (**Tables S3-S5**) are reported in the section 2 of the *Supplementary*
133 *material*.

134 2.3 Study design

135 The study was a randomized, single-blinded two-arms intervention of single intake of VM and
136 VC, involving twenty healthy voluntary subjects (11 males and 9 females aged between 25 and
137 60 years). The study followed the guidelines set by the Helsinki Declaration
138 (<http://www.fda.gov/ohrms/dockets/dockets/06d0331/06D-0331-EC20-Attach-1.pdf>) and all
139 subjects provided written informed consent prior to the study. Ethical approval for freeze-dried
140 VM and VC powdered supplement administration was obtained for a phase I-II study (approval
141 n. SPE 14.178 AOUC, 30th May 2016).

142 All the subjects convened early in the morning after 10 h of fasting and were randomly divided
143 in two groups according to an electronic randomisation key. A single dose of 25 g of VM
144 supplement mixed with 500 mL of water was orally administered to the first group, whereas
145 the same amount of VC berry supplement mixed with 500 mL of water was orally administered
146 to the second group. Serum was collected at baseline and different sampling times (30, 60, 120,
147 240 and 360 minutes) after the supplement assumption, as described in section 3 (**Table S6**) of
148 the *Supplementary material*. After the collection, samples were divided in aliquots of 500 μ L,
149 frozen at -80°C and stored until LC-HRMS analysis was performed.

2.4 Serum extraction

Serum extraction was performed on Waters Ostro 96-well plates as reported elsewhere (1). Quality of the untargeted analysis was guaranteed by the use of quality control (QC) samples and internal and external standards. See details in the section 4 of the *Supplementary material*.

2.5 LC-MS and LC-MS/MS analysis

LC analysis was performed on a Dionex (Sunnyvale, CA, USA) Ultimate 3000 HPLC system equipped with a Kinetex C18 column (150 mm x 2.1 mm I.D., particle size 2.6 μ m) and a guard column containing the same stationary phase (Phenomenex, Torrance, CA, USA). The LC system was coupled to a hybrid linear ion trap Fourier Transform (LTQ FT) Orbitrap high-resolution mass spectrometer (Thermo Fisher, Waltham, MA, USA) by an electrospray ionization (ESI) probe for MS and MS/MS analysis both in positive (PI) and negative (NI) ionization. Each sample was analysed under PI and NI, using two different mass acquisition methods for each ionization mode. The first method consisted of a Full Scan method (mass range from 100 to 1000 Da) at a mass resolution of 30,000 FWHM (m/z 400) in centroid mode. The second method included data dependent acquisition (DDA) scans for the three most abundant ions per scan at resolution of 7500 FWHM. Product ions were generated in the LTQ trap at collision energy of 35 eV using an isolation width of 2 Da. Further details related to MS acquisition are reported in the section 5 of the *Supplementary material*.

2.6 Data pre-treatment

All raw data were manually inspected using the Qual browser module of Xcalibur version 2.0.7 (Thermo Fisher). The LC-MS raw files were converted to mzML format using the MSConvert utility included in ProteoWizard (26). Then, the mzML files were processed with the *XCMS* R package that allows for obtaining detection and retention time alignment of features (i.e. ions characterized by a unique exact mass and retention time) (2, 27). During this processing, the maximum value for mass accuracy and retention time deviation was set equal to 5 ppm and 2

seconds, respectively. Data pre-processing of Full Scan acquisitions was performed according to Garcia-Aloy et al. 2020 (28). Briefly, each dataset was filtered to discard noisy and irrelevant features. Firstly, those features whose first decimal place took a value between 4 and 8 were removed from each data set. Subsequently, the signals that showed a higher variation coefficient in QC samples than within study samples were also excluded. A random number between 1 and 500 replaced all zero values. These thresholds were fixed empirically according to the intensity level representing the noise of the chromatogram. The principal component analysis (PCA) on log-transformed and Pareto-scaled data was applied to check data quality (i.e. possible batch effect) and to detect the presence of outliers.

2.7 Chemometrics analyses

PEMs in postprandial responses were selected separately for VM and VC interventions using a selection protocol consisting in a two-step procedure: i) statistical significance among time points within a same intervention and ii) nutrikinetic discrimination between interventions.

2.7.1 Statistical significance among time points of a same intervention

For the identification of PEMs suitable for the discrimination among time points, the following approaches were investigated: univariate post-hoc non-parametric Games-Howell and Wilcoxon signed-rank tests, univariate parametric *t*-test, and multivariate PLS-DA-VIP. A short overview of the characteristics of these tests is reported in section 6 of the *Supplementary material* (**Table S7**).

For the univariate approaches, we first selected those features with increasing mean values of chromatographic intensity in at least two consecutive time points, against baseline samples (i.e. time point “0 min”). Normal distribution of data was investigated by the application of Shapiro-Wilk’s test for multiple variables, while homogeneity of variance was evaluated adopting a Bartlett’s test for multiple independent variables, comparing the variances of VM and VC datasets in both polarities. Then, the *t*-test and the post-hoc non-parametric Games-Howell and

Wilcoxon tests were applied to evaluate the statistical significance between time point “0 min” and all the others, setting the threshold P -value at 0.05. For both t -test and non-parametric tests, the Benjamini-Hochberg procedure was applied to decrease the false discovery rate (significance level 5%).

The multivariate PLS-DA-VIP approach was performed on (i) the pre-treated VM and VC datasets and (ii) using the *plsda* package implemented with VIP scoring, setting the inclusion cut-off as > 1 , as elsewhere reported (11, 16).

2.7.2 VM and VC discrimination by nutrikinetic data

For each feature selected as significant in VM and/or VC, the baseline sample was subtracted from the intensities of the other time points, and in case of negative values, the replacement by zero was performed. Nutrikinetic significant features were selected using a two-step procedure based on their nutrikinetic curve behaviour. For that purpose, according to a previous intervention study (28), features that in at least two consecutive points exhibited the 25th percentile of one group ($n = 2$) higher than the 75th percentile of the other group ($n = 8$), were included in the discrimination process based on comparison of area under the curve (AUC). AUC of each selected feature was calculated between time 0 and 360 min using the *pracma* R package. Differences of AUCs among diets were tested using the Kruskal-Wallis test and the obtained P -values were adjusted using the Benjamini Hochberg method. Adjusted P -values < 0.05 were considered statistically significant. Descriptive analysis for evaluating the discrimination between the two interventions was carried out by means of PCA using the *FactoMineR* R package. Quality control of PCA was performed using QCs by visually verifying if PCA object scores obtained by replicated injections of the QC sample were close to the origin of PCA coordinates. Linear discriminant analysis (LDA) was performed on QC, VC, and VM sample groups made up by the annotated PEMs discriminating the two interventions, using the *MASS* R package.

2.8 Metabolite identification

The identification of features of interest, evidenced by data analysis, was performed according to the criteria previously reported by our research group (19), using the workflow described below. (i) Comparison of the exact mass of the experimental precursor ion with the pseudo-molecular ions proposed by the MzCloud (www.mzcloud.org), Humane Metabolome Database (HMDB, www.hmdb.ca), MassBank of North America (MoNA, <http://mona.fiehnlab.ucdavis.edu>), and Kyoto Encyclopedia of Genes and Genomes (KEGG) libraries, selecting a mass accuracy (Δ) ≤ 5 ppm as tolerance threshold. (ii) Export of the isotopic profile of pseudo-molecular ions selected within libraries at step (i) and subsequent comparison with the isotopic profile of the experimental precursor ions, selecting features providing an isotope ratio percentage difference of 20% as tolerance threshold. (iii) Structural elucidation of features of interest through the evaluation of MS/MS spectra obtained with DDA mass method in comparison with matched library mass spectra. (iv) Feature annotation performed according to golden standards for metabolomics (29).

3 Results and discussion

3.1 Assessment of data quality

Internal standards in study samples and QC samples showed a variation of retention time and mass accuracy below 2 seconds and 5 ppm, respectively, thus highlighting the correct data acquisition. Moreover, the variation of integrated area of the surrogate standards (added before the extraction) and internal standard (added before the analysis) in all the QC samples resulted lower than 20% confirming the repeatability of the extraction and excluding the possibility of signal drift and carry over phenomena during the LC-MS and LC-MS/MS analysis. Moreover, by means of Pareto-scaled PCA performed on raw data (data not shown), it was possible to observe that QC samples are well grouped in component space, showing no batch effect, or

249 trend due to the injection order (i.e. drop in signal intensity). Study samples are distributed
250 homogenously with no visible trends according to post-prandial time point.

251 3.2 Chemometrics workflow for feature selection

252 After data pre-treatment, complex data sets were obtained for both interventions, being the total
253 number of features 12091 and 5361 for PI and NI, respectively.

254 The supervised multivariate PLS-DA-VIP analysis was performed on these groups of features,
255 as commonly done in literature, highlighting a very high number of statistically significant
256 features (2283-8639, depending on the dataset considered). This result is probably due to the
257 tendency of the PLS-DA-VIP approach to select false positives. In fact, this criterion is very
258 reasonable to discard irrelevant variables, but it may have drawbacks if used for assessing the
259 significance of features (11). Moreover, model classification error rate of maximized distances
260 was very high, ranging from 0.9 to 0.7, regardless the number of selected components for PLS-
261 DA modelling.

262 For the application of univariate data analysis, the total number of features was preliminarily
263 filtered by a selection procedure that preserves only the features showing increasing intensities
264 in at least two consecutive time points. This feature selection resulted in a number of relevant
265 postprandial features ranging from 4245 to 4932, depending on the intervention and acquisition
266 mode (**Table 1**). The obtained datasets were checked for (i) normal distribution and (ii)
267 homogeneity of variance (i.e. homoscedasticity). Normality was evaluated by the application
268 of the Shapiro-Wilk's test for multiple variables. Shapiro-Wilk's correlation coefficients and
269 *P*-values (in bracket) ranged as follows: (i) VC – NI 0.538-0.897 ($1.0 \cdot 10^{-5}$ - $4.9 \cdot 10^{-2}$); (ii) VC –
270 PI 0.656-0.761 ($3.0 \cdot 10^{-3}$ - $4.9 \cdot 10^{-2}$); (iii) VM – NI 0.366-0.807 ($1.0 \cdot 10^{-7}$ - $3.4 \cdot 10^{-2}$); (iv) VM – PI
271 0.609-0.734 ($2.0 \cdot 10^{-4}$ - $5.0 \cdot 10^{-3}$), thus highlighting the absence of normality of the investigated
272 datasets. Homogeneity of variance was evaluated adopting the Bartlett's test for multiple
273 independent variables, comparing the variances of VC and VM datasets in both polarities. The

274 results obtained were characterized by P -value < 0.05 (confidence interval = 0.95), thus
275 evidencing lack of homogeneity among variances of the aforementioned datasets.

276 The aforementioned univariate tests were used for the PEMs selection within the
277 aforementioned datasets of relevant postprandial features, obtaining more or less populated
278 groups of statistically significant features in each acquisition polarity (**Table 1**). The adoption
279 of the t -test generated the largest group of “statistically significant” PEMs, which surely
280 includes a high number of false positives, even after the P -value correction using the
281 Benjamini-Hochberg procedure (1051-2154 features, depending on the dataset considered),
282 due to the non-normal and heteroscedastic distribution of data, which should discourage the
283 use of parametric test for PEMs selection. The Wilcoxon test was found to be much more
284 restrictive (75-359 features) than the adjusted t -test, in accordance with its non-parametric
285 character, which does not require compliance with the conditions of normality and
286 heteroscedasticity of data distribution, making it therefore more suitable for the treatment of
287 small sample size, for which the above-mentioned conditions usually do not occur. A
288 significantly reduced number of statistically significant features (i.e. 80 and 29 for VM and VC
289 interventions, respectively) was identified using the Games-Howell test, thus highlighting its
290 strong selectivity, which greatly reduces the probability of including false positives in the
291 PEMs group.

292 Using some features that can be annotated easily due to their previous identifications in bilberry
293 and/or blueberry intervention studies as representative cases, it is interesting to evaluate how
294 these features are treated by the procedures of PEMs selection here tested. For instance, benzoic
295 acid was annotated here ($\Delta = -0.4$ ppm) after the intake of VC supplement and retained in the
296 statistically significant PEMs group using the adjusted t -test. However, this feature was
297 excluded when PLS-DA-VIP or the non-parametric Wilcoxon and Games-Howell tests for
298 PEMs selection were applied. Moreover, hippuric acid was annotated here ($\Delta = -0.6$ ppm) in

both interventions and considered statistically significant by PLS-DA-VIP, adjusted *t*-test, and Wilcoxon test but excluded by the Games-Howell treatment. It is interesting to note that these features were considered statistically significant in a study investigating plasma after blueberry intake using ANOVA and post-hoc Bonferroni correction (24). As further examples, four metabolites (i.e. hydroxy-methoxy hippuric acid, hydroxy-(hydroxy-methoxyphenyl)-pentenoic acid glucuronide, dihydroxyphenyl propionic acid glucuronide, and hydroxyphenyl propionic acid sulphate) recently annotated as PEMs of bilberry intake (1), resulted here statistically significant by applying the Wilcoxon signed-rank test, while they were discarded by the Games-Howell test, due to the different assumptions made with respect to Wilcoxon test.

All these examples evidenced that the selection of significant features is strongly dependent on the statistical tool adopted. Based on these findings, great caution should be used in reporting metabolites as statistically significant for a given intervention. The application of highly conservative statistical methods, i.e. prone to minimizing the risk of false positive results is certainly useful in this sense and should be encouraged, although it involves a certain risk of excluding false negative from the significant dataset. On the contrary, the use of less restrictive tests should be used with great caution in PEMs discovery, even though they give a wider overview of features that could become significant when moving from a pilot study, i.e. characterized by a limited number of subjects, to one on a larger validation cohort.

3.3 PEMs annotation

Among the features selected by the Games-Howell test, corresponding to 47 PEMs, the annotation protocol allowed for identifying 5 features in PI and 13 features in NI, corresponding to a total of 12 PEMs. **Table 2** reports the annotated metabolites, providing their spectral characteristics, formula, time points for statistically significant maximum intensities (T_{\max}) with related *P*-values, the annotation level, and for annotation levels I and II, the

HMDB/KEGG identification numbers. Among the twelve PEMs identified, eight were annotated only after VM intervention (peaks 2-6, 9, 11, and 12), three only after VC ingestion (peaks 7, 8, and 10), and only one (peak 1) as common response to the consumption of the two supplements.

Peak 1 showed two pseudo-molecular ions in NI Full Scan spectra, i.e. at m/z 335.0504 and m/z 167.0214. The second ion was characterized by a fragmentation pattern that matched with uric acid, as reported in mzCloud spectral library and literature findings (30). **Peak 2** was putatively annotated as citric acid, due the occurrence of precursor ions at m/z 193.0335 and 191.0202, in PI and NI, respectively. MS/MS fragmentation pattern included as main fragments in NI mode peaks at m/z 173 (loss of a water molecule) and m/z 111.0091 (loss of acetic acid), whilst in PI m/z 132.1019 (loss of acetic acid) was highlighted. This attribution was confirmed by mzCloud spectral library and previous researches (31). **Peak 3** exhibited $[M-H]^-$ ion at m/z 267.0744, characterized by the neutral loss of 132 Da (pentose moiety) that led to the formation of a fragment at m/z 135.0313 associated to hypoxanthine, in accordance with spectral libraries and previous findings (32). Thus, this metabolite was putatively identified as inosine, a nucleoside naturally occurring in the pathway of purine metabolism after vegetable and/or fruit intake (33). **Peak 4** gave rise to a $[M-H]^-$ pseudo-molecular ion at m/z 194.0454 Da, which fragmented by losing 44 Da (CO_2) originating the fragment at m/z 150.0561. Since the pseudo-molecular ion matched with high accuracy ($\Delta=-2.6$ ppm) the mass of a hydroxy-hippuric acid and no other fragments were detected in the MS^2 spectrum, α -hydroxy-hippuric acid, p -hydroxy-hippuric acid, and o -hydroxy-hippuric acid reference standards were injected, obtaining t_R of 3.3, 3.8, and 5.4 minutes, respectively. Accordingly, peak 4 was annotated at level I as α -hydroxy-hippuric acid. **Peak 5** was putatively identified as benzodiol (catechol) sulphate owing to the presence of the typical loss of sulphate (m/z 79.9576) and the appearance of the hydroxy-phenol ion at m/z 109.0297 in the MS/MS spectrum (1, 34). An analogous

fragmentation pattern was observed for **peak 6**, putatively identified as methyl-catechol sulphate, due to the presence in the MS/MS spectrum of a peak at m/z 188.9860 (loss of methyl), together with typical losses of sulfonic (m/z 123.0454) and sulphate (m/z 108.0220) groups. **Peak 7** (PI: m/z 279.1329, NI: m/z 277.1185) and **peak 8** (PI: m/z 275.1024, NI: m/z 273.0875) were recognized as indole alkaloids derivatives, based on their mass accuracy and similar MSⁿ fragmentation patterns (**Figure S1** of the *Supplementary material*). Spectra of both peaks in PI (**Fig. S1, box A** and **box E**) were characterized by the neutral loss of C₂H₃NO₂ (73 Da, iminoacetic acid), typical of carboxylic acid derivatives of carboline (35). Moreover, under NI mode, the pseudo-molecular ions (i.e. m/z 277.1185 and 273.0875) underwent the sequential loss of two CO₂ moieties, indicating the presence of two carboxylic groups (**Fig. S1, box B-C** and **box F-G**). In order to confirm the attribution of **peaks 7** and **8** to the carboline class, their fragmentation patterns were compared with the one of 1-methyl-1,2,3,4-tetrahydro-β-carboline-3-carboxylic acid reference standard (**Fig. S1, boxes D-H**). Interestingly, the pseudo-molecular ion of **peak 8** in NI mode (m/z 273.0875) lost a carboxylic group, originating the feature at m/z 229.0982 (**Fig. S1, box F**), the fragmentation pattern of which (**Fig. S1, box G**) matched the one of the analytical standard 1-methyl-1,2,3,4-tetrahydro-β-carboline-3-carboxylic acid (**Fig. S1, box D**) with good mass accuracy and similar ions intensities. It should also be noted that **peak 7** showed in both PI (**Fig. S1, boxes A** vs. **E**) and NI (**Fig. S1, boxes B** vs. **F** and **C** vs. **G**) MSⁿ spectra a constant difference of about 4.03 Da compared to corresponding ions of **peak 8**. Hence, **peak 7** was annotated as octahydro-methyl-β-carboline-dicarboxylic acid. **Peak 9** showed the [M-H]⁻ pseudo-molecular ion in NI at m/z 439.1599, which fragmented through the typical neutral loss of glucuronide-conjugated compounds (176 Da) giving rise to the product ion at m/z 263.1288. This ion further fragmented originating the m/z 219.1391 and 153.0921 ions (**Figure S2-A** of the *Supplementary material*), which can be attributed to abscisic acid, as also highlighted by injecting the abscisic acid reference standard

(Figure S2-B). Peaks 10 and 11 were annotated as caprylic acid and azelaic acid, respectively, by comparing their mass spectra with those present in spectral databases (i.e. mzCloud and HMDB, see Table 2). In addition, azelaic acid was further confirmed at Level I by injecting the analytical standard. Finally, peak 12 was putatively annotated as hydroxy-phenyl propionic acid sulphate thanks to the mass accuracy of its $[M-H]^-$ pseudo-molecular ion (m/z 245.0119, $\Delta=-2.4$ ppm), the comparison with MS² spectral libraries, and based on findings of previous clinical studies on VM intake (1).

3.4 Nutrimetabolomics significance

The twelve annotated metabolites reported in Table 2 were categorized as (i) purine pathway metabolites, (ii) benzoic and benzodiol metabolites, (iii) indole alkaloids, and (iv) organic and fatty acids, according to their chemical class and metabolism. Figures 2-5 report the serum postprandial kinetics of the 12 annotated PEMs, expressed as boxplots of the precursor ion intensity as a function of time. Each boxplot represents the interquartile range (75% of the intensity values are less than or equal to the top value of the box and 25% of the intensity values are less than or equal to the bottom value of the box), the upper and lower whiskers refer to the maximum and minimum data point, respectively, and the line within the box represents the median of the data.

3.4.1 Purine pathway metabolites

Figure 2 illustrates the kinetic profile of the pseudo-molecular ions of uric acid (peak 1) in VM (Fig. 2A) and VC (Fig. 2B), and inosine (peak 3) in VM (Fig. 2C). According to literature, these metabolites are correlated with the ingestion of fructose, rather than phenolic compounds, since fructose induces acute depletion of ATP and inorganic phosphate and causes increased activity of the enzymes involved in the degradation of purine nucleotides to inosine, hypoxanthine, xanthine, and finally uric acid (36). Statistically significant variations ($P < 0.05$) of uric acid and inosine were observed at T_{\max} 30-60 min, suggesting that the fructose-induced

response increases uric acid concentration in plasma in the early stages of metabolism. The increase in uric acid is responsible of the raise of plasma antioxidant activity widely observed in literature after ingestion of fructose-rich fruits (33, 37). The fast depletion of these metabolites after two-three hours from food intake is in agreement with the post-prandial trend commonly observed for phase II metabolites of methylxanthines, which are rapidly excreted through the urinary trait within eight hours from the intake (38, 39).

3.4.2 Benzoic and benzodiol metabolites

Figure 3 shows the kinetic profiles of α -hydroxy-hippuric acid (**peak 4, Fig. 3A**), the sulphate derivatives of catechol (**peak 5, Fig. 3B**) and methyl-catechol (**peak 6, Fig. 3C**), and hydroxyphenyl propionic acid sulphate (**peak 12, Fig. 3D**), which were detected only in response to the VM intervention. Differently from purine derivatives, the trend observed for these compounds reflected a diverse postprandial scenario. In fact, the increase in signals intensities became statistically significant ($P < 0.05$) starting from two hours after the supplement ingestion (T_{\max} between 120 and 360 min), suggesting that their occurrence in plasma is associated to microbiota activity, which mediates the degradation of polyphenols in smaller and more soluble molecules (40). In detail, the occurrence in human plasma of both hippuric acid and catechol derivatives was already reported in literature (1, 23, 24) as potential markers of acute and/or long-term ingestion of bilberry and blueberry, and their occurrence related to quercetin glycosides, which are dominant flavonols in these fruits (1, 41, 42). Conversely, phenyl-propionic acid derivatives may derive from caffeic acid degradation and/or from anthocyanins after B-ring cleavage, and C-ring opening and oxidation (43).

3.4.3 Indole alkaloids

Figure 4 reports the kinetic profiles of the octahydro-methyl- β -carboline-dicarboxylic acid (**peak 7, Fig. 4A-B**) and the tetrahydro-methyl- β -carboline-dicarboxylic acid (**peak 8, Fig. 4C-D**), which have been annotated here for the first time in human plasma in response to the VC

intervention. Interestingly, both PEMs showed a significant increase in their intensities ($P < 0.05$) in plasma at T_{\max} 60 min, then decreasing in the following time points, suggesting that they are rapidly absorbed by human organism and likewise excreted through the urinary tract, as highlighted elsewhere (44). This group of chemicals is already known to occur in fruits, including berries, as well as in food processed products, suggesting that diet may directly contribute to their presence in human bio-fluids (35, 45, 46). However, the occurrence of these alkaloids should not be necessarily associated to the intake of fruit, since other foods such as beer, coffee, cereal products, and vegetables contain these alkaloids and may therefore contribute to their presence in human biofluids (35, 44).

3.4.4 Organic and fatty acids

Figure 5 illustrates the kinetic profiles observed in response to the VM intervention for citric acid (**peak 2, Fig. 5A-B**), abscisic acid glucuronide (**peak 9, Fig. 5C-D**), and azelaic acid (**peak 11, Fig. 5F**). Moreover, the trend of caprylic acid (**peak 10, Fig. 5E**) after VC intervention is also shown.

Citric acid showed a postprandial maximum intensity in between 30 and 60 min. Even though this compound is already known as one of the main organic acids occurring in various fruits, including blueberry and especially bilberry (47-49), these data represent the first evidence of a correlation between fruit intake and the occurrence of a statistically significant increase of citric acid in plasma.

Abscisic acid glucuronide reached a T_{\max} at 120 min after the supplement consumption, suggesting that it is involved in the phase II metabolism, even though the possible endogenous contribution associated with supplement intake cannot be excluded. In fact, abscisic acid has been found at relevant concentrations in bilberry fruits as a well-known plant hormone involved in the regulation of biosynthesis of polyphenols, such as anthocyanins (50).

Caprylic acid and azelaic acid showed a postprandial maximum intensity at very different T_{\max} , i.e. 30 min and 360 min after VC and VM interventions, respectively. In detail, caprylic acid, after the very fast absorption with an early post-prandial maximum intensity, exhibited a rapid decrease in the following time points, ascribable to its excretion by urine. On the other hand, the late intensity increase of the azelaic acid kinetic profile suggests a closer dependence on the phase I metabolism than the phase II one. The presence of fatty acids in serum has been poorly investigated in association with phenolic-rich fruit interventions. However, caprylic acid has been detected in human serum after pomegranate ingestion, probably due to its occurrence in seeds (51). Moreover, fatty acids other than caprylic and azelaic have been detected in human serum after the intake of mulberry and attributed to their occurrence in fruit seeds and peels (52). Hence, to our knowledge, caprylic acid and azelaic acid have been reported here as PEMs of VM and VC interventions for the first time.

3.5 Discrimination between VM and VC interventions

Comparison of serum metabolome profiles between the two berry interventions (performed according to the protocol described in section 2.7.2) showed ten and fifteen discriminant features in PI and NI, respectively, which correspond to thirteen PEMs. Among these, four metabolites matched the previously annotated PEMs, i.e. abscisic acid glucuronide, α -hydroxy-hippuric acid, catechol sulphate, and methyl-catechol sulphate, which were found to be statistically significant in VM intervention (**Table 2**).

In order to provide a summarising description of the discrimination capacity between the two interventions by the thirteen PEMs, it is interesting to perform a multivariate analysis by means of PCA and LDA of the autoscaled intensity data of these PEMs, expressed as the highest intensity value determined for each feature under NI in the kinetic profile of each intervention. Moreover, the intensities of these PEMs in QC samples were included in both PCA and LDA, in order to make more informative the multivariate analyses, also avoiding misclassifications.

Five principal components (PCs) characterized by eigenvalues > 1 and accounting for percentages of explained variance (EV) of 29.9%, 12.9%, 12.2%, 11.2%, and 8.2% were obtained (total EV=74.6%).

Table S8 in section 6 of the *Supplementary material* illustrates the loading values of the five significant PCs. Most features mainly contributed to only one PC with high absolute values of the loadings, thus highlighting a good separation of the original variables among PCs. For example, abscisic acid glucuronide, α -hydroxy-hippuric acid, catechol sulphate, methylcatechol sulphate, and the unknown at m/z 287.0224 contributed significantly only to PC1, which alone accounts for about a third of the total variance of the original data. A detailed description of the contribution of the various features to the five significant PCs is reported in section 6 of the *Supplementary material*. **Figure 6** illustrates the score plots of PC1 vs. PC2, PC3, PC4, and PC5, which highlights a quite good separation of QC, VC, and VM samples in all the four PC spaces. Moreover, QCs were very close to the origin of the coordinates, suggesting a high accuracy and precision of the entire analytical procedure. LDA has been also carried out on the dataset of the discriminating PEMs in QC, VC, and VM samples, in order to verify the correct assignment of each sample to its own group (i.e. QC, VM, and VC). The summary of the results obtained for the fitted and cross-validated (leave-one-out method) LDA classification are illustrated in **Table 3**. QC samples were correctly classified in all cases, both in fitting and in cross-validation, thus evidencing the robustness of this classification and confirming the results of PCA regarding the reliability of the analytical procedure here adopted. The LDA classification exhibited a very high robustness also for the VM and VC groups, since all samples were correctly classified in fitting and only two (i.e. one for each intervention) were misclassified in cross-validation. It should however be remarked that the two misclassified samples were attributed to the QC group, without any misleading attribution to the other volunteer group.

498 4 Conclusions

499 The comparative evaluation of different multivariate and univariate methods for PEMs
500 selection evidenced that the number of significant features is strongly dependent on the
501 statistical tool adopted, thus highlighting the importance of testing multiple statistical
502 approaches for PEMs discovery.

503 The protocol of untargeted metabolomics analysis and chemometrics data treatment adopting
504 the non-parametric Games-Howell test for PEMs selection within interventions, was suitable
505 for selecting a restricted set of statistically significant features, excluding a number of false
506 positive, which were conversely retained in the highly populated group of “significant
507 features”, generated by other statistical methods, commonly adopted in literature. Accordingly,
508 this chemometrics strategy could be fruitfully extended to the data treatment of intervention
509 studies characterized by a similar study design (i.e. small sample size, randomized, single-
510 blinded, parallel studies). In fact, it is more useful to identify a smaller set of PEMs, accepting
511 a certain risk of excluding from this group some significant metabolites (false negatives), rather
512 than selecting a larger group of PEMs, which however contains a high number of false positive.
513 It should also be noted that with the presented approach it is possible to concentrate the
514 annotation effort on a smaller but highly discriminant and certainly significant set of PEMs.

515 Twelve PEMs related to the intake of bilberry and/or blueberry supplements were annotated in
516 serum samples, five of them (i.e. octahydro-methyl- β -carboline-dicarboxylic acid and
517 tetrahydro-methyl- β -carboline-dicarboxylic acid for VC, citric acid for VM, and caprylic acid
518 and azelaic acid for both VC and VM) reported here for the first time as serum metabolites of
519 these interventions.

520 Based on AUC analysis, thirteen PEMs were found statistically significant for the
521 discrimination of VM and VC interventions. In this regard, it is remarkable that this group of
522 PEMs included four intra-intervention relevant metabolites (i.e. abscisic acid glucuronide,

catechol sulphate, methyl-catechol sulphate, and α -hydroxy-hippuric acid), thus confirming the validity of the selection workflow based on the Games-Howell test. PCA data exploration and LDA samples classification performed on PEMs intensity at T_{\max} corroborating the discriminating role of the thirteen PEMs.

Acknowledgements

The authors wish to acknowledge the support of the Regione Toscana and the private companies Il Baggiolo S.r.l., Danti Giampiero & C. S.n.c., Azienda Agricola Il Sottobosco, and Farmaceutica MEV S.r.l., through the PRAF Misura 1.2. e) grant.

Conflict of interest

The authors declare that they have no conflict of interest.

References

1. Ancillotti C, Ulaszewska M, Mattivi F, Del Bubba M. Untargeted metabolomics analytical strategy based on liquid chromatography/electrospray ionization linear ion trap quadrupole/orbitrap mass spectrometry for discovering new polyphenol metabolites in human biofluids after acute ingestion of vaccinium myrtillus berry supplement. *J Am Soc Mass Spectrom.* 2019;30(3):381-402.
2. Ulaszewska M, Garcia-Aloy M, Vázquez-Manjarrez N, Soria-Florido M, Llorach R, Mattivi F, et al. Food intake biomarkers for berries and grapes. *Genes Nutr.* 2020;15(1):1-35.
3. Koutsos A, Riccadonna S, Ulaszewska MM, Franceschi P, Trošt K, Galvin A, et al. Two apples a day lower serum cholesterol and improve cardiometabolic biomarkers in mildly hypercholesterolemic adults: a randomized, controlled, crossover trial. *Am J Clin Nutr.* 2020;111(2):307-18.
4. Lacalle-Bergeron L, Izquierdo-Sandoval D, Sancho JV, López FJ, Hernández F, Portolés T. Chromatography hyphenated to high resolution mass spectrometry in untargeted metabolomics for investigation of food (bio) markers. *TrAC, Trends Anal Chem.* 2020;116:161.
5. Ulaszewska MM, Weinert CH, Trimigno A, Portmann R, Andres Lacueva C, Badertscher R, et al. Nutrimetabolomics: an integrative action for metabolomic analyses in human nutritional studies. *Mol Nutr Food Res.* 2019;63(1):1800384.
6. Stanstrup J, Broeckling CD, Helmus R, Hoffmann N, Mathé E, Naake T, et al. The metaRbolomics Toolbox in Bioconductor and beyond. *Metabolites.* 2019;9(10):200.
7. Hendriks MM, van Eeuwijk FA, Jellema RH, Westerhuis JA, Reijmers TH, Hoefsloot HC, et al. Data-processing strategies for metabolomics studies. *TrAC, Trends Anal Chem.* 2011;30(10):1685-98.
8. Cuparencu CS, Andersen M-BS, Gürdeniz G, Schou SS, Mortensen MW, Raben A, et al. Identification of urinary biomarkers after consumption of sea buckthorn and strawberry, by untargeted LC-MS metabolomics: a meal study in adult men. *Metabolomics.* 2016;12(2):31.
9. Xu T, Feng G, Zhao B, Zhao J, Pi Z, Liu S, et al. A non-target urinary and serum metabolomics strategy reveals therapeutical mechanism of Radix Astragali on adjuvant-induced arthritis rats. *J Chromatogr B.* 2017;1048:94-101.

10. Dickson L, Tenon M, Svilar L, Fança-Berthon P, Martin J-C, Rogez H, et al. Genipap (*Genipa americana* L.) juice intake biomarkers after medium-term consumption. *Food Res Int*. 2020;137:109375.
11. Cocchi M, Biancolillo A, Marini F. Chemometric methods for classification and feature selection. *Comprehensive Analytical Chemistry*. 82: Elsevier; 2018. p. 265-99.
12. Vinaixa M, Samino S, Saez I, Duran J, Guinovart JJ, Yanes O. A guideline to univariate statistical analysis for LC/MS-based untargeted metabolomics-derived data. *Metabolites*. 2012;2(4):775-95.
13. Banaszewski K, Park E, Edirisinghe I, Cappozzo JC, Burton-Freeman BM. A pilot study to investigate bioavailability of strawberry anthocyanins and characterize postprandial plasma polyphenols absorption patterns by Q-TOF LC/MS in humans. *J Berry Res*. 2013;3(2):113-26.
14. Medina S, Ferreres F, Garcia-Viguera C, Horcajada M-N, Orduna J, Saviron M, et al. Non-targeted metabolomic approach reveals urinary metabolites linked to steroid biosynthesis pathway after ingestion of citrus juice. *Food Chem*. 2013;136(2):938-46.
15. Franceschi P, Giordan M, Wehrens R. Multiple comparisons in mass-spectrometry-based-omics technologies. *TrAC, Trends Anal Chem*. 2013;50:11-21.
16. Lamichhane S, Sen P, Dickens AM, Hyötyläinen T, Orešič M. An overview of metabolomics data analysis: current tools and future perspectives. *Comprehensive analytical chemistry*. 2018;82:387-413.
17. Godzien J, Ciborowski M, Angulo S, Barbas C. From numbers to a biological sense: How the strategy chosen for metabolomics data treatment may affect final results. A practical example based on urine fingerprints obtained by LC-MS. *Electrophoresis*. 2013;34(19):2812-26.
18. Manach C, Scalbert A, Morand C, Rémésy C, Jiménez L. Polyphenols: food sources and bioavailability. *Am J Clin Nutr*. 2004;79(5):727-47.
19. Ancillotti C, Ciofi L, Rossini D, Chiuminatto U, Stahl-Zeng J, Orlandini S, et al. Liquid chromatographic/electrospray ionization quadrupole/time of flight tandem mass spectrometric study of polyphenolic composition of different *Vaccinium* berry species and their comparative evaluation. *Anal Bioanal Chem*. 2017;409(5):1347-68.
20. Patel S. Blueberry as functional food and dietary supplement: The natural way to ensure holistic health. *Mediterr J Nutr Metab*. 2014;7(2):133-43.
21. Del Bubba M, Di Serio C, Renai L, Scordo CVA, Checchini L, Ungar A, et al. *Vaccinium myrtillus* L. extract and its native polyphenol-recombined mixture have anti-proliferative and pro-apoptotic effects on human prostate cancer cell lines. *Phytother Res*. 2020;35(2):1089-98.
22. Thomasset S, Berry DP, Cai H, West K, Marczylo TH, Marsden D, et al. Pilot study of oral anthocyanins for colorectal cancer chemoprevention. *Cancer Prev Res*. 2009;2(7):625-33.
23. Feliciano RP, Istas G, Heiss C, Rodriguez-Mateos A. Plasma and urinary phenolic profiles after acute and repetitive intake of wild blueberry. *Molecules*. 2016;21(9):1120.
24. Rodriguez-Mateos A, Feliciano RP, Cifuentes-Gomez T, Spencer JP. Bioavailability of wild blueberry (poly) phenols at different levels of intake. *J Berry Res*. 2016;6(2):137-48.
25. Ancillotti C, Ciofi L, Pucci D, Sagona E, Giordani E, Biricolti S, et al. Polyphenolic profiles and antioxidant and antiradical activity of Italian berries from *Vaccinium myrtillus* L. and *Vaccinium uliginosum* L. subsp. *gaultherioides* (Bigelow) SB Young. *Food Chem*. 2016;204:176-84.
26. Chambers MC, Maclean B, Burke R, Amodei D, Ruderman DL, Neumann S, et al. A cross-platform toolkit for mass spectrometry and proteomics. *Nat Biotechnol*. 2012;30(10):918-20.

27. Ulaszewska MM, Trost K, Stanstrup J, Tuohy KM, Franceschi P, Chong MF-F, et al. Urinary metabolomic profiling to identify biomarkers of a flavonoid-rich and flavonoid-poor fruits and vegetables diet in adults: the FLAVURS trial. *Metabolomics*. 2016;12(2):32.
28. Garcia-Aloy M, Ulaszewska M, Franceschi P, Estruel-Amades S, Weinert CH, Tor-Roca A, et al. Discovery of Intake Biomarkers of Lentils, Chickpeas and White Beans by Untargeted LC-MS Metabolomics in Serum and Urine. *Mol Nutr Food Res*. 2020;1901137.
29. Sumner LW, Amberg A, Barrett D, Beale MH, Beger R, Daykin CA, et al. Proposed minimum reporting standards for chemical analysis. *Metabolomics*. 2007;3(3):211-21.
30. Kim KM, Henderson GN, Ouyang X, Frye RF, Sautin YY, Feig DI, et al. A sensitive and specific liquid chromatography–tandem mass spectrometry method for the determination of intracellular and extracellular uric acid. *J Chromatogr B*. 2009;877(22):2032-8.
31. Li C-R, Hou X-H, Xu Y-Y, Gao W, Li P, Yang H. Manual annotation combined with untargeted metabolomics for chemical characterization and discrimination of two major crataegus species based on liquid chromatography quadrupole time-of-flight mass spectrometry. *J Chromatogr A*. 2020;1612:460628.
32. Lv Y, Liu X, Yan S, Liang X, Yang Y, Dai W, et al. Metabolomic study of myocardial ischemia and intervention effects of Compound Danshen Tablets in rats using ultra-performance liquid chromatography/quadrupole time-of-flight mass spectrometry. *J Pharm Biomed Anal*. 2010;52(1):129-35.
33. Jakše B, Jakše B, Pajek M, Pajek J. Uric acid and plant-based nutrition. *Nutrients*. 2019;11(8):1736.
34. Liu H, Garrett TJ, Su Z, Khoo C, Gu L. UHPLC-Q-Orbitrap-HRMS-based global metabolomics reveal metabolome modifications in plasma of young women after cranberry juice consumption. *J Nutr Biochem*. 2017;45:67-76.
35. Vázquez-Manjarrez N, Ulaszewska M, Garcia-Aloy M, Mattivi F, Praticò G, Dragsted LO, et al. Biomarkers of intake for tropical fruits. *Genes Nutr*. 2020;15(1):1-21.
36. Lotito SB, Frei B. Consumption of flavonoid-rich foods and increased plasma antioxidant capacity in humans: cause, consequence, or epiphenomenon? *Free Radical Biol Med*. 2006;41(12):1727-46.
37. Godycki-Cwirko M, Krol M, Krol B, Zwolinska A, Kolodziejczyk K, Kasielski M, et al. Uric acid but not apple polyphenols is responsible for the rise of plasma antioxidant activity after apple juice consumption in healthy subjects. *J Am Coll Nutr*. 2010;29(4):397-406.
38. Martínez-López S, Sarriá B, Gómez-Juaristi M, Goya L, Mateos R, Bravo-Clemente L. Theobromine, caffeine, and theophylline metabolites in human plasma and urine after consumption of soluble cocoa products with different methylxanthine contents. *Food Res Int*. 2014;63:446-55.
39. Oracz J, Nebesny E, Zyzelewicz D, Budryn G, Luzak B. Bioavailability and metabolism of selected cocoa bioactive compounds: A comprehensive review. *Crit Rev Food Sci Nutr*. 2020;60(12):1947-85.
40. Pimpao RC, Ventura MR, Ferreira RB, Williamson G, Santos CN. Phenolic sulfates as new and highly abundant metabolites in human plasma after ingestion of a mixed berry fruit puree. *Br J Nutr*. 2015;113(3):454-63.
41. Bresciani L, Martini D, Mena P, Tassotti M, Calani L, Brigati G, et al. Absorption profile of (poly) phenolic compounds after consumption of three food supplements containing 36 different fruits, vegetables, and berries. *Nutrients*. 2017;9(3):194.
42. Jaganath IB, Jaganath IB, Mullen W, Edwards CA, Crozier A. The relative contribution of the small and large intestine to the absorption and metabolism of rutin in man. *Free Radical Res*. 2006;40(10):1035-46.
43. Nurmi T, Mursu J, Heinonen M, Nurmi A, Hiltunen R, Voutilainen S. Metabolism of berry anthocyanins to phenolic acids in humans. *J Agric Food Chem*. 2009;57(6):2274-81.

- 661 44. Hövelmann Y, Lewin L, Steinert K, Hübner F, Humpf HU. Mass Spectrometry-Based
662 Analysis of Urinary Biomarkers for Dietary Tomato Intake. *Mol Nutr Food Res.*
663 2020;64(12):2000011.
- 664 45. Herraiz T. Analysis of the bioactive alkaloids tetrahydro- β -carboline and β -carboline
665 in food. *J Chromatogr A.* 2000;881(1-2):483-99.
- 666 46. Koleva II, van Beek TA, Soffers AE, Dusemund B, Rietjens IM. Alkaloids in the human
667 food chain—natural occurrence and possible adverse effects. *Mol Nutr Food Res.*
668 2012;56(1):30-52.
- 669 47. Akagić A, Oras AV, Oručević Žuljević S, Spaho N, Drkenda P, Bijedić A, et al.
670 Geographic Variability of Sugars and Organic Acids in Selected Wild Fruit Species. *Foods.*
671 2020;9(4):462.
- 672 48. Mikulic-Petkovsek M, Schmitzer V, Slatnar A, Stampar F, Veberic R. Composition of
673 sugars, organic acids, and total phenolics in 25 wild or cultivated berry species. *J Food Sci.*
674 2012;77(10):C1064-C70.
- 675 49. Phillips MM, Case RJ, Rimmer CA, Sander LC, Sharpless KE, Wise SA, et al.
676 Determination of organic acids in Vaccinium berry standard reference materials. *Anal Bioanal*
677 *Chem.* 2010;398(1):425-34.
- 678 50. Karppinen K, Hirvelä E, Nevala T, Sipari N, Suokas M, Jaakola L. Changes in the
679 abscisic acid levels and related gene expression during fruit development and ripening in
680 bilberry (*Vaccinium myrtillus* L.). *Phytochemistry.* 2013;95:127-34.
- 681 51. Medjakovic S, Jungbauer A. Pomegranate: a fruit that ameliorates metabolic syndrome.
682 *Food Funct.* 2013;4(1):19-39.
- 683 52. Zhang H, Ma ZF, Luo X, Li X. Effects of mulberry fruit (*Morus alba* L.) consumption
684 on health outcomes: A mini-review. *Antioxidants.* 2018;7(5):69.

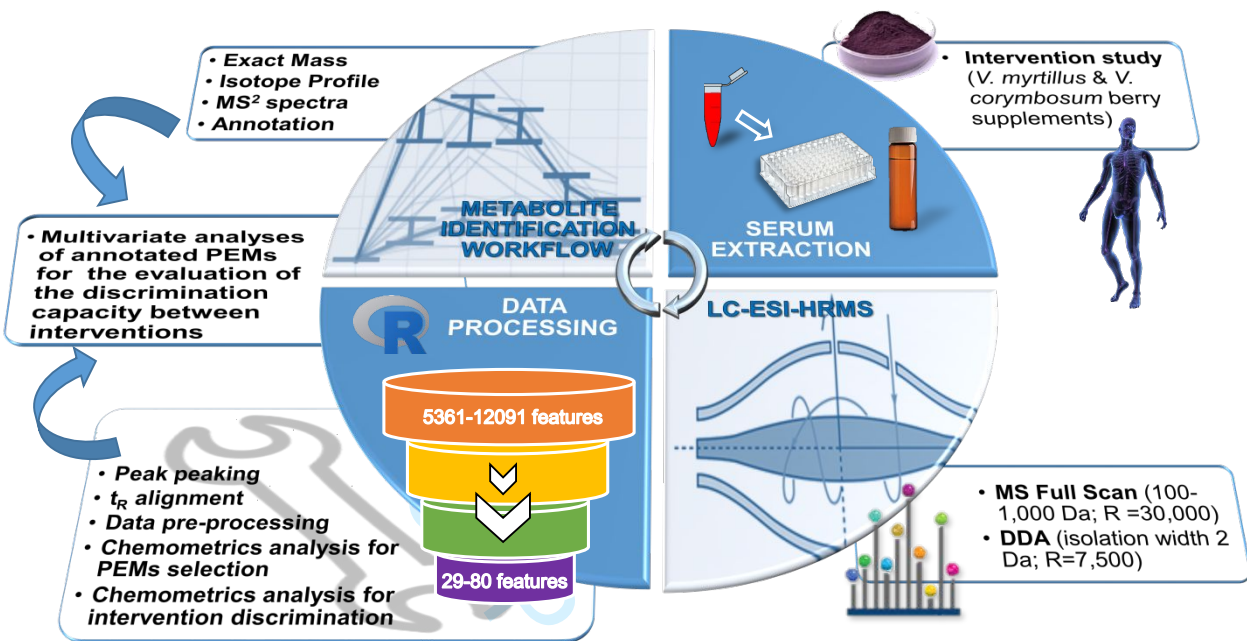


Figure 1 – Graphical workflow of the experimental steps followed in this study.

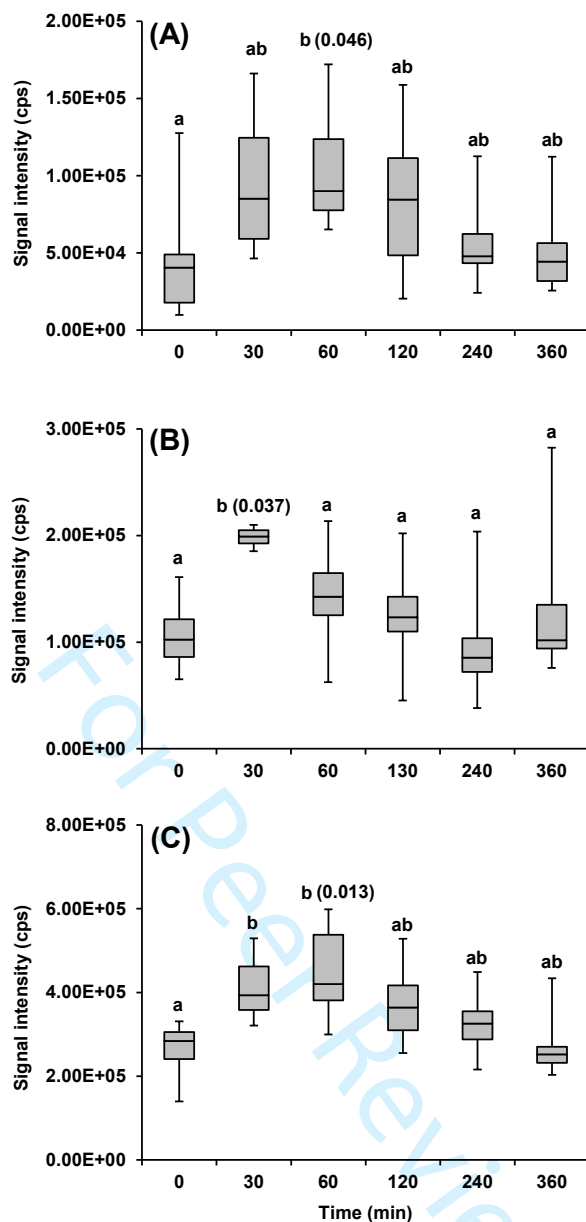


Figure 2 – Kinetic profiles of the pseudo-molecular ions (negative ionization mode) at m/z (A) 335.0504 (uric acid in VM), (B) 167.0214 (uric acid in VC), and (C) 267.0744 (inosine in VM). Boxplots exhibiting different letters are significantly different according to the Games-Howell comparison test ($P < 0.05$). T_{\max} of each pseudo-molecular ion is labelled in bracket with its corresponding P -value.

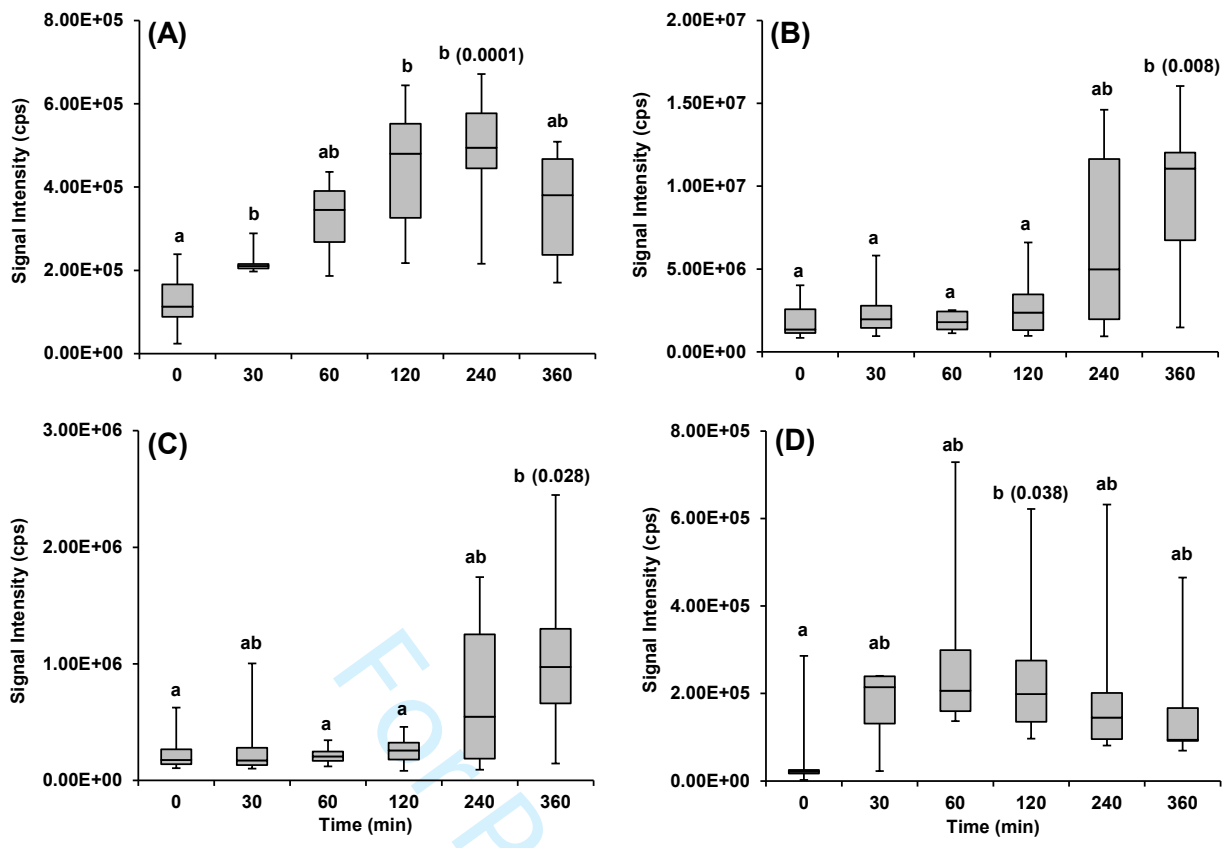


Figure 3 – Kinetic profiles of the pseudo-molecular ions (negative ionization mode) at m/z (A) 194.0454 (α -hydroxy-hippuric acid in VM), (B) 188.9856 (catechol sulphate in VM), (C) 203.0014 (methyl-catechol sulphate in VM), and (D) 245.0119 (hydroxyphenyl propionic acid sulphate in VM). Boxplots exhibiting different letters are significantly different according to the Games-Howell comparison test ($P < 0.05$). T_{\max} of each pseudo-molecular ion is labelled in bracket with its corresponding P -value.

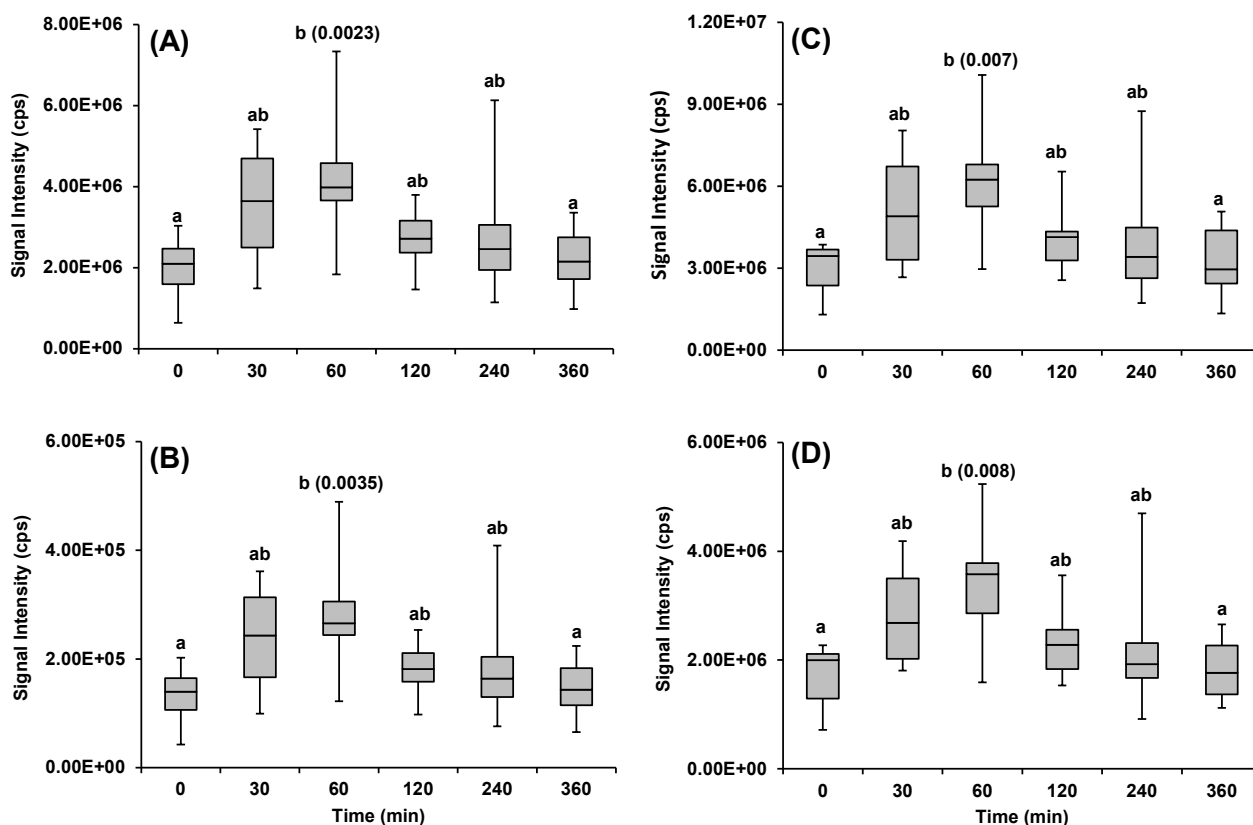


Figure 4 – Kinetic profiles of the pseudo-molecular ions (positive and negative ionization, respectively) at m/z (A) 279.1329 and (B) 277.1185 (octahydro-methyl- β -carboline-dicarboxylic acid in VC), (C) 275.1024 and (D) 273.0875 (tetrahydro-methyl- β -carboline-dicarboxylic acid in VC). Boxplots exhibiting different letters are significantly different according to the Games-Howell comparison test ($P < 0.05$). T_{\max} of each pseudo-molecular ion is labelled in bracket with its corresponding P -value.

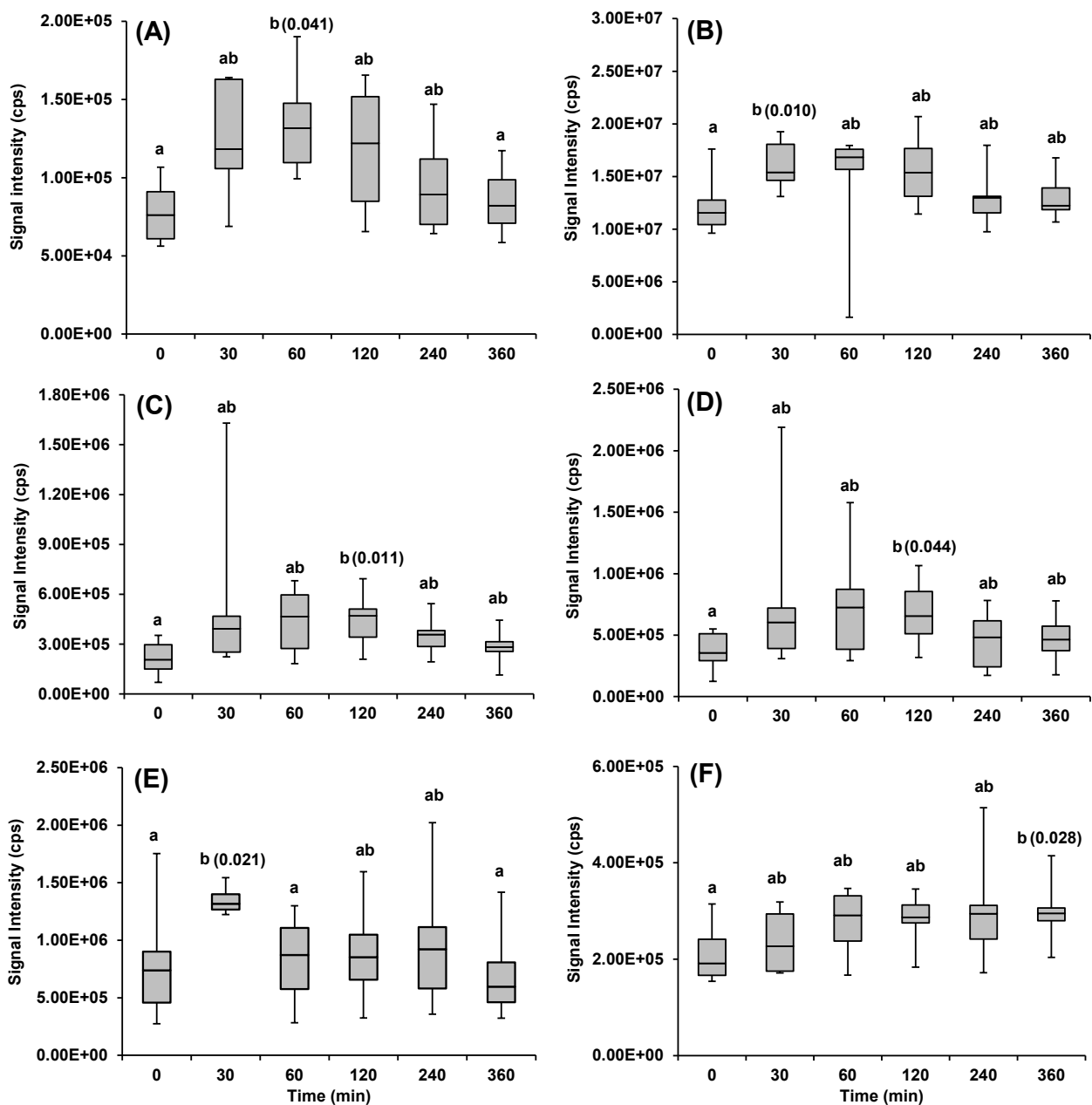


Figure 5 – Kinetic profiles of the pseudo-molecular ions at m/z (A) 191.0202 and (B) 193.0335 (citric acid in VM under negative and positive ionization, respectively), (C) 265.1431 and (D) 439.1599 (abscisic acid glucuronide in VM under positive and negative ionization, respectively), (E) 145.1220 (caprylic acid in VC under positive ionization), and (F) 187.0980 (azelaic acid in VM under negative ionization). Boxplots exhibiting different letters are significantly different according to the Games-Howell comparison test ($P < 0.05$). T_{\max} of each pseudo-molecular ion is labelled in bracket with its corresponding P -value.

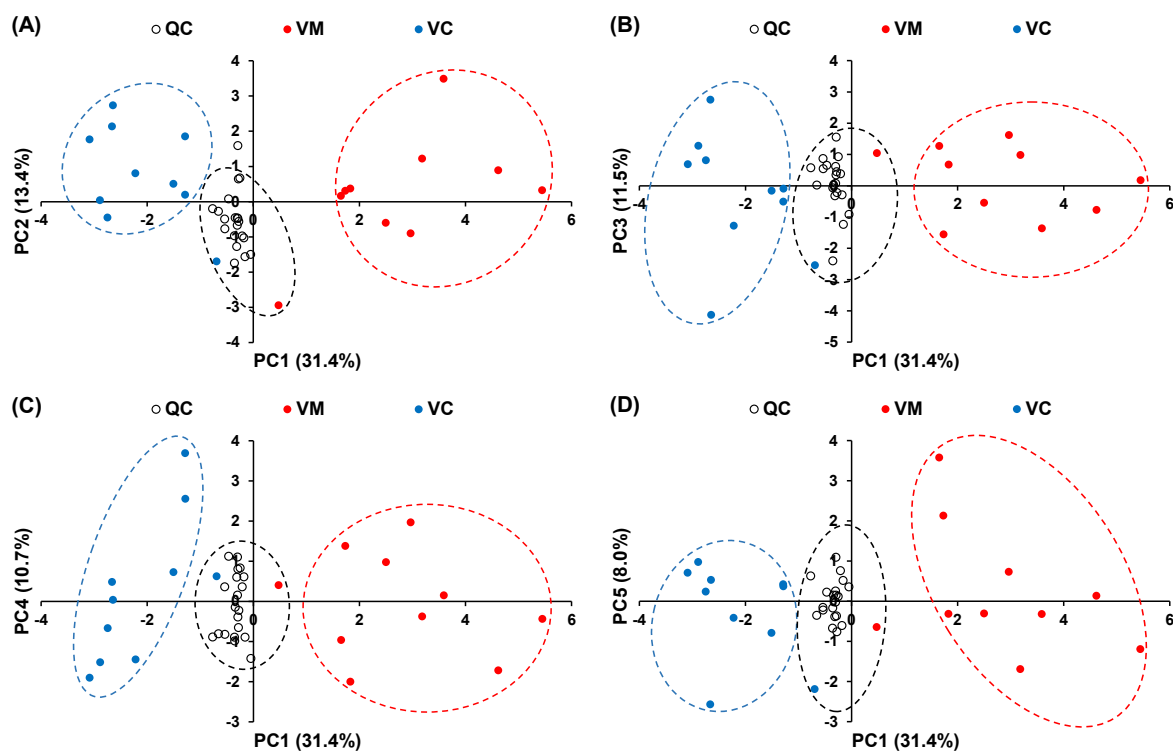


Figure 6 – Score plots of (A) PC1 vs. PC2, (B) PC1 vs. PC3, (C) PC1 vs. PC4, and (D) PC1 vs. PC5. PCA plots were obtained using the autoscaled intensity data of the PEMs discriminating the two interventions in serum samples from each volunteer, expressed as their features measured under NI at the maximum of their kinetic profile in each intervention. Ellipses identify samples assigned to the QC, VM, and VC groups by applying linear discriminant analysis of maximum intensity of each annotated PEMs after cross validation with the leave-one-out method.

1
2
3
4
5
6
7
8
9
10
11
12
13
14
15
16
17
18
19
20
21
22
23
24
25
26
27
28
29
30
31
32
33
34
35
36
37
38
39
40
41
42
43
44
45
46
47
48
49
50
51
52
53
54
55
56
57
58
59
60

Table 1 — Number of relevant postprandial features and potential exposure markers (PEMs) in each dataset (intervention and acquisition polarity) identified using the selection strategies based on univariate non-parametric adjusted post-hoc Games-Howell test, pairwise Wilcoxon signed-rank test and the univariate parametric *t*-Test, before and after the Benjamini-Hochberg adjustment procedure (BH-adj). VM = *Vaccinium myrtillus* supplement intervention; VC = *Vaccinium corymbosum* supplement intervention.

Dataset	Relevant postprandial features	<i>t</i> -test	BH-adj	Wilcoxon	Games-Howell
VM ESI (+)	4731	4682	1957	359	29
VC ESI (+)	4932	4395	2154	146	18
VM ESI (–)	4655	3286	1075	224	51
VC ESI (–)	4245	2582	1051	75	11

For Peer Review

Table 2 — List of metabolites found in serum samples after acute ingestion of *V. myrtillus* (VM) and *V. corymbosum* (VC) supplements. Retention time (t_R , min), experimental mass in Full Scan spectrum (Da), main MS/MS fragments (base peak in bold), proposed formula, mass accuracy (Δ , ppm), time point of max intensity (T_{max} , min) and P -value within interventions (in brackets), and HMDB/KEGG identification numbers. Roman numbers refer to the level of annotation: (I) spectra and t_R matched with reference standard; (II) spectra matched with reference libraries; (III) spectra matched with literature information. n.a.= not available.

Peak	t_R	Full Scan	MS/MS	Formula	T_{max} (P -value)	Identification	HMDB/KEGG
1	1.2	\ominus 335.0504 [2M-H] ⁻ \ominus 167.0214	167.0214 124.0156 , 96.0207	C ₅ H ₄ N ₄ O ₃	VM: 60 min (0.046) VC: 30 min (0.037)	Uric acid ^(II)	HMDB0000289/C00366
2	1.2	\oplus 193.0335 [M+H] ⁺ \ominus 191.0202 [M-H] ⁻	132.1019 173.0093, 111.0091	C ₆ H ₈ O ₇	VM: 30 min (0.041) VM: 60 min (0.010)	Citric acid ^(II)	HMDB0000094/C00158
3	1.5	\ominus 267.0744 [M-H] ⁻	135.0313	C ₁₀ H ₁₂ N ₄ O ₅	VM: 60 min (0.013)	Inosine ^(II)	HMDB0000195/C00294
4	3.1	\ominus 194.0454 [M-H] ⁻	150.0561	C ₉ H ₉ NO ₄	VM: 240 min (0.0001)	α -Hydroxy-hippuric acid ^(I)	HMDB0013678 HMDB0006116
5	3.9	\ominus 188.9856 [M-H] ⁻	109.0297	C ₆ H ₆ O ₅ S	VM: 360 min (0.008)	Benzendiol (catechol) sulphate ^(II)	HMDB0059724
6	4.7	\ominus 203.0014 [M-H] ⁻	188.9860, 123.0454 , 108.0220	C ₇ H ₈ O ₅ S	VM: 360 min (0.028)	Methyl-catechol sulphate ^(II)	HMDB0240663
7	5.23	\oplus 279.1329 [M+H] ⁺ \ominus 277.1185 [M-H] ⁻ \ominus 233.1232	235.1376, 206.1110, 163.1165 233.1232 189.1336 , 187.1179, 146.0914, 120.0759, 96.0736	C ₁₄ H ₁₈ N ₂ O ₄	VC: 60 min (0.023 ⁽⁺⁾ , 0.035 ⁽⁻⁾)	Octahydro-methyl- β -carboline-dicarboxylic acid ^(III)	n.a.
8	5.30	\oplus 275.1024 [M+H] ⁺ \oplus 202.0861 \ominus 273.0875 [M-H] ⁻ \oplus 229.0982	231.1128, 202.0861, 159.0916 184.0755 , 156.0802 229.0982 185.1084 , 183.0928, 142.0663, 116.0508, 92.0508,	C ₁₄ H ₁₄ N ₂ O ₄	VC: 60 min (0.007 ⁽⁺⁾ , 0.008 ⁽⁻⁾)	Tetrahydro-methyl- β -carboline-dicarboxylic acid ^(II)	HMDB0035115
9	5.9	\oplus 265.1431 \oplus 247.1326 \ominus 439.1599 [M-H] ⁻	247.1329 , 199.1023 229.1431, 211.1327 263.1288 , 219.1395, 175.0248, 153.0922	C ₂₁ H ₂₈ O ₁₀	VM: 120 min (0.044)	Absciscic acid glucuronide ^(II)	HMDB0036093 HMDB0035140
10	6.3	\oplus 145.1220 [M+H] ⁺	127.1130 , 109.1008	C ₈ H ₁₆ O ₂	VC: 30 min (0.021)	Caprylic acid (hydroxy-octanone) ^(II)	HMDB00482/ HMDB0062511 HMDB62511/C06423
11	6.4	\ominus 187.0980 [M-H] ⁻	125.0973	C ₉ H ₁₆ O ₄	VM: 360 min (0.028)	Azelaic acid ^(I)	HMDB00784/C08261
12	6.5	\ominus 245.0119 [M-H] ⁻	165.0556	C ₉ H ₁₀ O ₆ S	VM: 120 min (0.038)	Hydroxyphenyl propionic acid sulphate ^(II)	HMDB0094710

1
2
3
4
5
6
7
8
9
10
11
12
13
14
15
16
17
18
19
20
21
22
23
24
25
26
27
28
29
30
31
32
33
34
35
36
37
38
39
40
41
42
43
44
45
46
47
48
49
50
51
52
53
54
55
56
57
58
59
60

Table 3 – Fitting (FIT) and cross-validation (CV) results of the Linear Discriminant Analysis based on the values of intensity data of the thirteen discriminating PEMs in serum samples from each volunteer, expressed as their features measured at the maximum of their kinetic profile in each intervention. Groups: quality control (QC), intervention with *Vaccinium corymbosum* supplement (VC), and intervention with *Vaccinium myrtillus* supplement (VM).

Put into Group		True Group		
		QC	VC	VM
QC	FIT	20	0	0
	CV	20	1	1
VC	FIT	0	10	0
	CV	0	9	0
VM	FIT	0	0	10
	CV	0	0	9
Total Number of Samples		20	10	10
Correct Attributions	FIT	20	10	10
	CV	20	9	9
Percentage of Correct Attribution	FIT	100%	100%	100%
	CV	100%	90%	90%

Manuscript: “Comparison of chemometrics workflows for potential exposure markers discovery and false positive reduction in untargeted metabolomics: application to the serum analysis by LC-HRMS after intake of *Vaccinium* fruits supplements” by L. Renai et al.

SUPPLEMENTARY MATERIAL

1 Supplement preparation

The supplements were obtained by cryo-milling separately 5-kg aliquots of bilberries and blueberries (Laboratorio Terapeutico M.R., Florence, Italy), which were freeze-dried not later than one week after fruit harvesting, so as to maintain as much as possible the berry native composition. In the period between harvest and freeze-drying the fruits were kept at -20°C. Both supplements appeared as very homogeneous powders, characterized by a significant degree of hygroscopicity and were therefore kept at -20°C in polyethylene food storage containers, until their use.

2 Supplement characterization

In order to assess the amount of total soluble polyphenols (TSP), total monomeric anthocyanins (TMA) and the most important phenolic compounds commonly found in bilberries and blueberries, the following protocols were adopted.

2.1 Supplement extraction

About 500 mg aliquots of supplement were homogenized in an ice bath under magnetic stirring with 15 mL of a methanol/water solution 8/2 (v/v) containing 10 mM NaF to inactivate polyphenol oxidase; the mixture was centrifuged at 1800xg for 5 min and the supernatant recovered. This procedure was repeated twice and the extracts combined and analysed for TSP, TMA, and selected phenolic compounds.

2.2 Analysis of TSP

TSP were spectrophotometrically determined as following described. Extract aliquots (100-200 µL, depending on the TSP concentration in the extract) were mixed with 200 µL of Folin-Ciocalteu reagent. After 3 min, 400 µL of an aqueous solution saturated with sodium carbonate were added and the mixture obtained was made up to 10 mL with ultra-pure water. The solution was dark incubated for 1 h. Afterwards, the absorbance was measured at 740 nm and TSP concentration calculated on the basis of a catechin calibration curve; accordingly, the results were expressed as milligrams of catechin/g of supplement.

2.3 Analysis of TMA

TMA were determined with the pH differential method using cyanidin-3-glucoside as reference standard. Aliquots of 100-200 μ L of extract were diluted in buffer solutions at pH=1 and pH=4.5, so as to obtain a final volume of 10 mL. The absorbance (Abs) of both solutions were measured at 520 and 700 nm and the quantity “ Δ Abs” was calculated according to equation 1.

$$\Delta\text{Abs} = (\text{Abs}_{\text{pH}=1}^{520\text{ nm}} - \text{Abs}_{\text{pH}=1}^{700\text{ nm}}) - (\text{Abs}_{\text{pH}=4.5}^{520\text{ nm}} - \text{Abs}_{\text{pH}=4.5}^{700\text{ nm}}) \quad (1)$$

Similarly, “ Δ Abs” values were also calculated for different concentrations of cyanidin-3-glucoside reference standard and plotted as a function of corresponding cyanidin-3-glucoside concentrations. The equation best fitting the experimental data was calculated by the least square regression method, thus obtaining a linear calibration curve, which was used for measuring TMA in the extracts. The results were expressed as milligrams of cyanidin-3-glucoside per g of supplement.

2.4 HPLC-MS/MS analysis of selected phenolic compounds

The following polyphenolic compounds were investigated: cyanidin-3-galactoside (CYA-3-GAL), cyanidin-3-glucoside (CYA-3-GLU), cyanidin-3-arabinoside (CYA-3-ARA), delphinidin-3-glucoside (DEL-3-GLU), delphinidin-3-galactoside (DEL-3-GAL), delphinidin-3-rabinoside (DEL-3-ARA), malvidin-3-glucoside (MAL-3-GLU), malvidin-3-galactoside (MAL-3-GAL), malvidin-3-arabinoside (MAL-3-ARA), peonidin-3-glucoside (PEO-3-GLU), peonidin-3-galactoside (PEO-3-GAL), peonidin-3-arabinoside (PEO-3-ARA), petunidin-3-glucoside (PET-3-GLU), petunidin-3-galactoside (PET-3-GAL), petunidin-3-arabinoside (PET-3-ARA), gallic acid (GAL), caffeic acid (CAF), p-coumaric acid (COU), ferulic acid (FER), salicylic acid (SAL), chlorogenic acid (CHL), neochlorogenic acid (NEO), cryptochlorogenic acid (CRY), (+)-catechin (CAT), epicatechin (EPI), procyanidin A2 (PA2), procyanidin B1 (PB1), procyanidin B2 (PB2) procyanidin C1 (PC1), kaempferol-3-glucoside (KAE-3-GLU), myricetin (MYR), quercetin (QUE), quercetin-3-galactoside (QUE-3-GAL), quercetin-3-glucoside (QUE-3-GLU), quercetin-3-rhamnoside (QUE-3-RHA), quercetin-3-rutinoside (QUE-3-RUT).

The analysis of phenolic compounds was carried out on the extracts after removal of organic solvent by vacuum evaporation, followed by acidification with formic acid up to pH = 2.0 ± 0.1 and filtration at 0.2 μ m on nylon membranes.

HPLC–MS/MS analysis was performed on an Acquity BEH C18 column (150 x 2.1 mm i.d.; particle size 1.7 μ m) equipped with a guard column containing the same stationary phase (Waters, Milford, MA, USA), using a Shimadzu (Kyoto, Japan) chromatographic system consisting of a low pressure gradient quaternary pump Nexera X2 LC-30AD, a CTO/20AC thermostatted column compartment, a SIL-30AC autosampler, a DGU-20A 5R degassing unit and a CBM-20A module controller. The

UHPLC system was coupled with a 5500 QTrapTM mass spectrometer (ABSciex, Ontario, Canada) by a Turbo VTM interface equipped with an electrospray probe. Chromatograms were elaborated by the 1.6.1 release of the software Analyst (AB Sciex).

Chromatographic analysis of anthocyanins was performed at 50°C with water/formic acid 95:5 v/v (eluent A) and methanol/formic acid 95:5 v/v (eluent B) according to the following gradient: 0.1-10 min linear gradient 7-17% B, 10-20 min linear gradient 17-22% B, 20-22 min linear gradient 22-95% B, 22-27 min isocratic 95% B.

Chromatographic analysis of phenolic acids, flavanols and flavonols was performed at 55°C, by eluting with water/formic acid 99.9:0.1 v/v (eluent A) and methanol/formic acid 99.9:0.1 v/v (eluent B) according to the following gradient: 0.1-1 min isocratic 4% B, 1-20 min linear gradient 4-70.5% B, 20-20.5 min linear gradient 70.5-95% B, 20.5-25 min isocratic 95% B.

The flow rate was 0.3 mL/min and the injection volume was 5 µL for both chromatographic analyses. Polyphenol MS/MS analysis was carried out using the Multiple Reaction Monitoring mode by ESI both in negative (for phenolic acids, flavanols and flavonols) and positive mode (for anthocyanins). For each investigated compound, the most intense transition was used for quantification and the second most intense for confirming identification. Compound dependent parameters were optimized by direct infusion of properly diluted target analyte standard solutions (**Tables S1** and **S2**). The quantification of DEL-3-ARA, PET-3-GAL, PET-3-ARA and MAL-3-ARA was performed in respect to the corresponding glucoside because of the absence of commercial standards.

Source dependent parameters were optimized in flow injection analysis at optimal LC flow and mobile phase composition. For negative ion determination optimal source dependent parameters were as follows: Curtain Gas 40, CAD Gas Medium, Temperature 550°C, Gas 1 60, Gas 2 40, Interface Heater ON and IonSpray Voltage -4500 V. For positive ion determination optimal source dependent parameters were as follows: Curtain Gas 40, CAD Gas Medium, Temperature 500°C, Gas 1 40, Gas 2 30, Interface Heater ON and IonSpray Voltage 5500 V.

1
2
3
4
5
6
7
8
9
10
11
12
13
14
15
16
17
18
19
20
21
22
23
24
25
26
27
28
29
30
31
32
33
34
35
36
37
38
39
40
41
42
43
44
45
46
47
48
49
50
51
52
53
54
55
56
57
58
59
60

Table S1 - Optimized MS parameters for the investigated anthocyanins. Letters A and B after each compound name refer to the quantifier and qualifier transitions, respectively. (DP) declustering potential; (EP) entrance potential; (CE) collision energy; (CXP) collision cell exit potential.

Compound	Precursor Ion (m/z)	Product Ion (m/z)	DP (V)	EP (V)	CE (V)	CXP (V)
SAL-A	137	93	-45	-7	-25	-10
SAL-B	137	65	-45	-7	-43	-20
GAL-A	169	125	-50	-9	-20	-11
GAL-B	169	137	-50	-9	-28	-15
COU-A	163	119	-50	-8	-20	-11
COU-B	163	93	-50	-8	-45	-10
CAF-A	179	135	-65	-10	-25	-12
CAF-B	179	134	-65	-10	-35	-10
FER-A	193	134	-50	-10	-20	-12
FER-B	193	149	-50	-10	-15	-14
CHL-A	353	191	-170	-13	-25	-20
CHL-B	353	85	-170	-13	-60	-10
NEO-A	353	191	-70	-8	-25	-25
NEO-B	353	179	-70	-8	-25	-20
CRY-A	353	173	-60	-8	-22	-25
CRY-B	353	179	-60	-8	-23	-20
CAT-A	289	245	-15	-9	-20	-20
CAT-B	289	109	-15	-9	-35	-10
EPI-A	289	245	-15	-9	-20	-20
EPI-B	289	109	-15	-9	-35	-10
PA2-A	575	285	-130	-8	-40	-25
PA2-B	575	289	-130	-8	-35	-20
PB1-A	577	289	-140	-7	-35	-30
PB1-B	577	407	-140	-7	-35	-20
PB2-A	577	289	-80	-7	-35	-30
PB2-B	577	407	-80	-7	-35	-25
PC1-A	865	407	-160	-7	-55	-30
PC1-B	865	289	-160	-7	-52	-25
KAE-3-GLU-A	447	284	-35	-8	-37	-12
KAE-3-GLU-B	447	255	-35	-8	-53	-15
MYR-A	317	151	-120	-8	-32	-15
MYR-B	317	179	-120	-8	-30	-15
QUE-A	301	151	-20	-7	-30	-14
QUE-B	301	179	-20	-7	-27	-17
QUE-3-GAL-A	463	300	-120	-8	-37	-15
QUE-3-GAL-B	463	271	-120	-8	-58	-15
QUE-3-GLU-A	463	300	-120	-8	-37	-15
QUE-3-GLU-B	463	271	-120	-8	-57	-15
QUE-3-RUT-A	609	300	-20	-5	-52	-15
QUE-3-RUT-B	609	271	-20	-5	-75	-15
QUE-3-RHA-A	447	300	-120	-8	-35	-15
QUE-3-RHA-B	447	271	-120	-8	-60	-15

Table S2 - Optimized MS parameters for the investigated polyphenols. Letters A and B after each compound name refer to the quantifier and qualifier transitions respectively. (DP) declustering potential; (EP) entrance potential; (CE) collision energy; (CXP) collision cell exit potential.

Compound	Precursor Ion (m/z)	Product Ion (m/z)	DP (V)	EP (V)	CE (V)	CXP (V)
DEL-3-GLU-A	465	303	110	10	40	25
DEL-3-GLU-B	465	229	110	10	75	25
DEL-3-GAL-A	465	303	110	10	40	25
DEL-3-GAL-B	465	229	110	10	75	25
CYA-3-GAL-A	449	287	100	10	40	25
CYA-3-GAL-B	449	137	100	10	75	15
CYA-3-GLU-A	449	287	120	10	40	20
CYA-3-GLU-B	449	137	120	10	75	12
CYA-3-ARA-A	419	287	90	12	35	25
CYA-3-ARA-B	419	137	90	12	70	15
PET-3-GLU-A	479	317	100	10	35	25
PET-3-GLU-B	479	302	100	10	60	25
PEO-3-GAL-A	463	301	100	10	35	20
PEO-3-GAL-B	463	286	100	10	55	25
PEO-3-GLU-A	463	301	100	10	35	20
PEO-3-GLU-B	463	286	100	10	55	25
PEO-3-ARA-A	433	301	100	10	35	20
PEO-3-ARA-B	433	286	100	10	55	25
MAL-3-GAL-A	493	331	120	8	35	15
MAL-3-GAL-B	493	315	120	8	65	15
MAL-3-GLU-A	493	331	110	9	35	20
MAL-3-GLU-B	493	315	110	9	65	20

2.5 Phenolic compounds concentrations in the supplements

Concentrations of TSP and TMA (**Table S3**), anthocyanins (**Table S4**) and other phenolic compounds (**Table S5**) determined in *V. myrtillus* and *V. corymbosum* supplements are reported below.

Table S3 – Total soluble polyphenol (TSP) and total monomeric anthocyanin (TMA) concentrations of *V. myrtillus* and *V. corymbosum* supplements administered to volunteers during the study.

	<i>V. myrtillus</i> supplement	<i>V. corymbosum</i> supplement
TSP (mg CAT/g supplement dry weight)	38.8 ± 2.1	9.3 ± 1.0
TMA (mg CYA-3-GLU/g supplement dry weight)	30.1 ± 2.8	6.4 ± 0.9

Table S4 –Targeted anthocyanin concentrations expressed as mg/g dry weight of *V. myrtillus* and *V. corymbosum* supplements.

Anthocyanins	<i>V. myrtillus</i> supplement	<i>V. corymbosum</i> supplement
DEL-3-GAL	4.07 ± 0.05	0.57 ± 0.04
DEL-3-GLU	4.24 ± 0.08	0.14 ± 0.05
DEL-3-ARA	2.90 ± 0.04	0.37 ± 0.02
CYA-3-GAL	3.69 ± 0.08	0.12 ± 0.01
CYA-3-GLU	3.04 ± 0.09	0.04 ± 0.01

CYA-3-ARA	2.27 ± 0.08	0.06 ± 0.01
PET-3-GAL	0.92 ± 0.04	0.42 ± 0.02
PET-3-GLU	2.29 ± 0.03	0.17 ± 0.02
PET-3-ARA	0.74 ± 0.04	0.26 ± 0.03
PEO-3-GAL	0.27 ± 0.02	0.07 ± 0.01
PEO-3-GLU	1.10 ± 0.07	0.03 ± 0.01
PEO-3-ARA	0.16 ± 0.01	0.03 ± 0.01
MAL-3-GAL	0.94 ± 0.04	1.69 ± 0.06
MAL-3-GLU	2.36 ± 0.05	0.63 ± 0.02
MAL-3-ARA	0.56 ± 0.02	1.28 ± 0.05

Table S5 – Targeted phenolic acid, flavanol and flavonol concentrations expressed as µg/g dry weight of *V. myrtillus* and *V. corymbosum* supplements.

Phenolic acids	<i>V. myrtillus</i> supplement	<i>V. corymbosum</i> supplement
GAL	41.6 ± 1.5	7.72 ± 0.8
p-COU	4.12 ± 0.05	0.58 ± 0.06
CAF	9.02 ± 0.2	3.96 ± 0.3
FER	0.93 ± 0.01	6.06 ± 0.07
SAL	0.61 ± 0.02	0.44 ± 0.03
CHL	2793 ± 35	796 ± 5
NEO	0.75 ± 0.08	3.38 ± 0.09
CRY	1.58 ± 0.05	1.50 ± 0.01
Flavanols	<i>V. myrtillus</i> supplement	<i>V. corymbosum</i> supplement
CAT	23.3 ± 0.9	17.0 ± 0.2
EPI	224 ± 16	235 ± 15
PA2	3.7 ± 0.4	0.18 ± 0.05
PB1	5.2 ± 0.4	10.1 ± 0.7
PB2	198 ± 21	5.3 ± 0.6
PC1	17.2 ± 0.8	3.2 ± 0.4
Flavonols	<i>V. myrtillus</i> supplement	<i>V. corymbosum</i> supplement
MYR	57.9 ± 1.3	3.88 ± 1.2
QUE	11.5 ± 0.1	5.93 ± 0.3
QUE-3-GAL	640 ± 38	268 ± 18
QUE-3-GLU	77.8 ± 1.4	69.2 ± 1.2
QUE-3-RHA	33.9 ± 1.0	43.4 ± 1.2
QUE-3-RUT	1.64 ± 0.21	58.8 ± 0.5
KAE-3-GLU	1.92 ± 0.08	4.64 ± 0.07

3 Study design

Volunteers participating to the study were divided in two groups depending on the supplement to be administered, which were indexed as VM and VC group, for *V. myrtillus* and *V. corymbosum*, respectively. Serum of each volunteer was collected at baseline and at different sampling times (30, 60, 120, 240 and 360 minutes) after the supplement taking and the name of each sample group was reported in **Table S6**.

Table S6 – Groups and sampling time used for statistical comparison serum samples.

Group Name	Sampling Time	Berry type
VM 0min	Baseline	<i>V. myrtillus</i>
VM 30min	30 minutes after supplement taking	<i>V. myrtillus</i>
VM 60min	60 minutes after supplement taking	<i>V. myrtillus</i>
VM 120min	120 minutes after supplement taking	<i>V. myrtillus</i>
VM 240min	240 minutes after supplement taking	<i>V. myrtillus</i>
VM 360min	360 minutes after supplement taking	<i>V. myrtillus</i>
VC 0min	Baseline	<i>V. corymbosum</i>
VC 30min	30 minutes after supplement taking	<i>V. corymbosum</i>
VC 60min	60 minutes after supplement taking	<i>V. corymbosum</i>
VC 120min	120 minutes after supplement taking	<i>V. corymbosum</i>
VC 240min	240 minutes after supplement taking	<i>V. corymbosum</i>
VC 360min	360 minutes after supplement taking	<i>V. corymbosum</i>

4 Serum extraction

As regards serum samples, the precipitation of proteins and the removal of phospholipids were performed using the Ostro 96-well plate (Waters, Milford, MA, USA). In detail, for each sample, 100 μL of serum were placed into the well and 100 μL of surrogate standards in methanol (12.5 $\mu\text{g/mL}$ TRI-d5 and HIP-d5) were added. Then, 300 μL of the first cold solvent (acetonitrile/formic acid 99:1 v/v) were added to each well, the system was covered and the well plate/collection plate were firstly mixed for 5 minutes and then placed on the positive pressure processor for the filtration (60 psi for 10 minutes). This procedure was repeated after the addition of 400 μL of the second cold solvent (acetonitrile/water 3:1 v/v with the 1% of formic acid). The resulting solutions were dried under nitrogen flow and re-diluted in 250 μL of the internal standard solution (0.42 $\mu\text{g/mL}$ CIN-d5). The resulting serum extracts were transferred in labelled brown vials for LC-MS analysis. For testing the serum extraction procedure, quality control (QC) samples were prepared, by mixing same volumes of all serum samples. Deuterated analytical standards were added to all QC samples and study samples to check for mass accuracy and drift of retention time. The same extraction protocol was performed on these quality control samples randomly placed in the well plate. The QC extracts together with the extraction blanks were injected before the analysis of study samples in both ionization modes. The QC samples were acquired each ten samples during LC-MS and LC-MS/MS analysis in both ionization modes.

1
2
3
4
5
6
7
8
9
10
11
12
13
14
15
16
17
18
19
20
21
22
23
24
25
26
27
28
29
30
31
32
33
34
35
36
37
38
39
40
41
42
43
44
45
46
47
48
49
50
51
52
53
54
55
56
57
58
59
60

5 LC-MS and LC-MS/MS analysis

The chromatographic analysis was performed on a Kinetex C18 column (150 mm x 2.1 mm I.D., particle size 2.6 μm) and a guard column containing the same stationary phase (Phenomenex, Torrance, CA, USA). Column temperature was set at 40°C. Water (eluent A) and acetonitrile (eluent B), both with 0.1 % formic acid, were used as mobile phases according to the following gradient: 0-1 min isocratic 5% B, 1-7 min linear gradient 5-45% B, 7-8.5 min linear gradient 45-80% B, 8.5-10.5 min isocratic 80% B. The flow rate was 350 $\mu\text{L}/\text{min}$ and the injection volume was 5 μL .

The ESI conditions in positive (and negative) mode were: spray voltage 5.0 kV (-3.5 kV), heated capillary temperature 320°C, capillary voltage 35 V (-35 V) and tube lens 110 V (-110 V).

In the LTQ component of the instrument, nitrogen was used as both the sheath gas (35 U) and auxiliary gas (5 U), and helium was used as the damping gas. All measurements were done using the automatic gain control of the LTQ to adjust the number of ions entering the trap. Mass calibration was performed with every sequence run just prior to starting the batch by using flow injection of the manufacturer’s calibration standards mixture allowing for mass accuracies lower than 5 ppm in external calibration mode.

6 Chemometrics

6.1 Statistical methods for inter-intervention selection of potential exposure markers (PEMs)

Table S7 – Brief overview of the statistical approaches and methods used in this study to test inter-intervention PEMs selection.

Methods for PEMs selection	Description
PLS-DA VIP	Combination of the multivariate linear regression technique PLS-R with discriminant classification. Variable importance in projection (VIP) scores are defined for each X variable as the sum of the PLS-weight value, weighted by the percentage of \hat{y} (or Y) variance.
(paired) <i>t</i> -test	Parametric test used to compare the means of two paired groups.
Wilcoxon Signed-rank test	Non-parametric alternative of paired <i>t</i> -test, used to determine whether the mean ranks of two dependent samples were selected from populations having the same distribution.
Post-hoc Games-Howell	Non-parametric post-hoc test to compare combinations of groups of data ($n > 2$), which does not assume equal variances and sample sizes, as well as normal distribution of data, since it works on ranked variables.

6.2 Principal component analysis of features discriminating the two interventions

The loadings obtained with principal component analysis of the thirteen features found to be significant for the discrimination of interventions are shown in **Table S8**. High and positive loadings were found on PC1 for α -hydroxy-hippuric acid, catechol sulphate, methyl-catechol sulphate, and the unknown at m/z 287.0224, which were well differentiated from abscisic acid glucuronide, the latter exhibiting a high but negative projection on this PC. The unknown at m/z 427.2535 and 643.3681 significantly contributed only to PC2 with negative and positive loadings, respectively. PC3 was mainly represented by the positive loading of the unknown at m/z 158.9390 and 420.0832, and the negative loadings of the unknowns at m/z 385.2375 and 465.2845. The unknown at m/z 273.9592 (positive loading) and 381.2306 (negative loading) were those exhibiting a much higher contribution to PC4. Both these features significantly contributed with negative loadings also to PC5, which was however represented by m/z 158.9390 (negative loading) and 420.0832 (positive loading).

Table S8 – Loading values of the thirteen features found to be statistically significant for the discrimination of the VM and VC interventions. Loading more representative of each PC are in bold.

Features	PC1	PC2	PC3	PC4	PC5
Abscisic acid glucuronide	-0.328	0.277	-0.154	0.174	-0.165
α -Hydroxy hippuric acid	0.423	-0.084	0.054	0.079	0.317
Methyl-cathecol sulphate	0.427	-0.097	-0.025	-0.127	-0.268
Cathecol sulphate	0.448	0.133	0.050	-0.108	-0.227
420.0832	-0.072	0.229	0.342	-0.216	0.510
158.9390	-0.138	0.224	0.471	0.123	-0.411
465.2845	-0.140	0.266	-0.457	0.289	0.157
427.2535	0.051	-0.534	-0.182	-0.355	-0.030
287.0224	0.423	0.134	-0.063	0.086	0.061
385.2375	0.052	0.275	-0.587	-0.220	0.080
643.3681	0.219	0.537	0.075	-0.081	0.005
273.9592	0.176	-0.183	-0.151	0.504	-0.348
381.2306	-0.153	0.126	-0.113	-0.590	-0.404

7 Annotation process

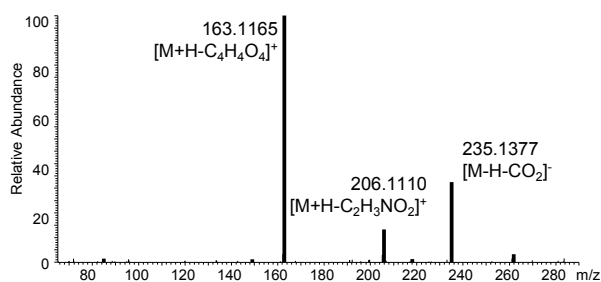
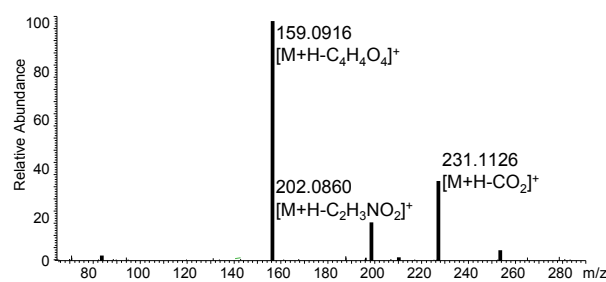
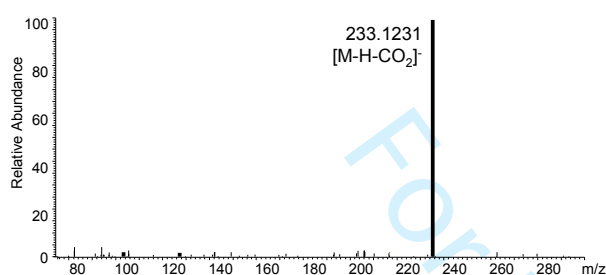
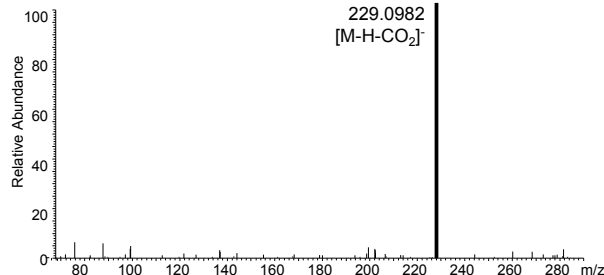
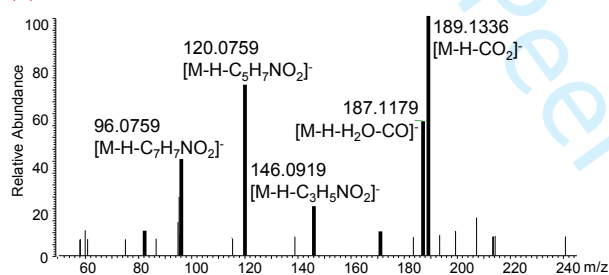
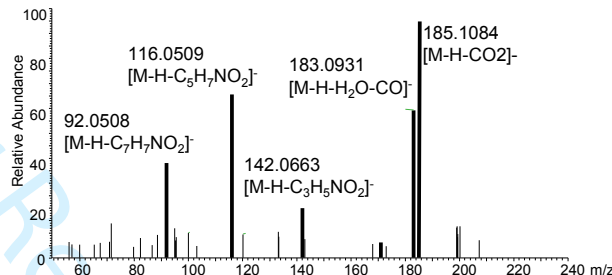
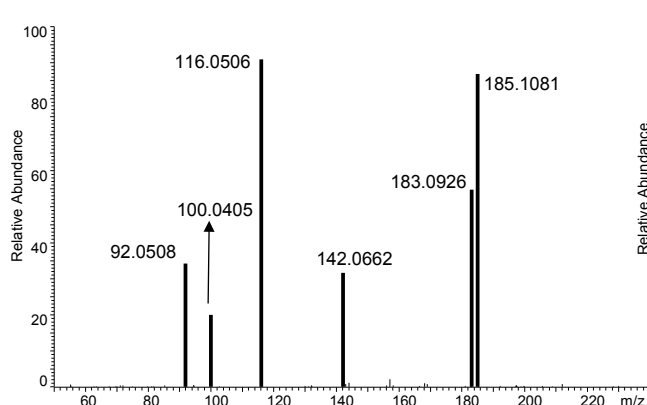
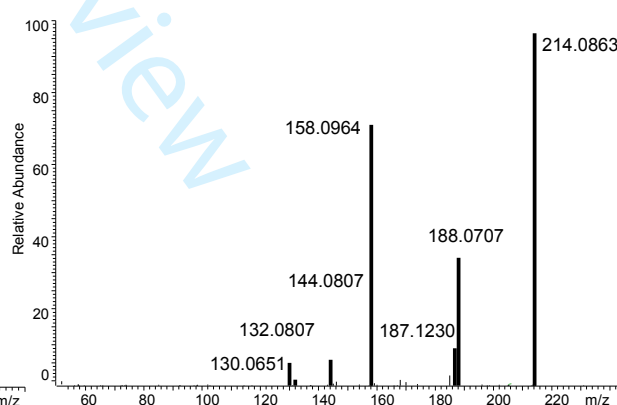
(A) FTMS POS MS² 279.1329(E) FTMS POS MS² 275.1024(B) FTMS NEG MS² 277.1185(F) FTMS NEG MS² 273.0875(C) FTMS NEG MS² 233.1232(G) FTMS NEG MS² 229.0982(D) NEG MS² 229.0978(H) POS MS² 331.1128

Figure S1 – Fragmentation patterns of peak 7 (boxes A, B, and C), annotated as octahydro-methyl- β -carboline-dicarboxylic acid, peak 8 (boxes E, F, and G), annotated as tetrahydro-methyl- β -carboline-dicarboxylic acid, and analytical standard of the carbolines reference compound 1-methyl-1,2,3,4-tetrahydro- β -carboline-3-carboxylic acid (boxes D and H).

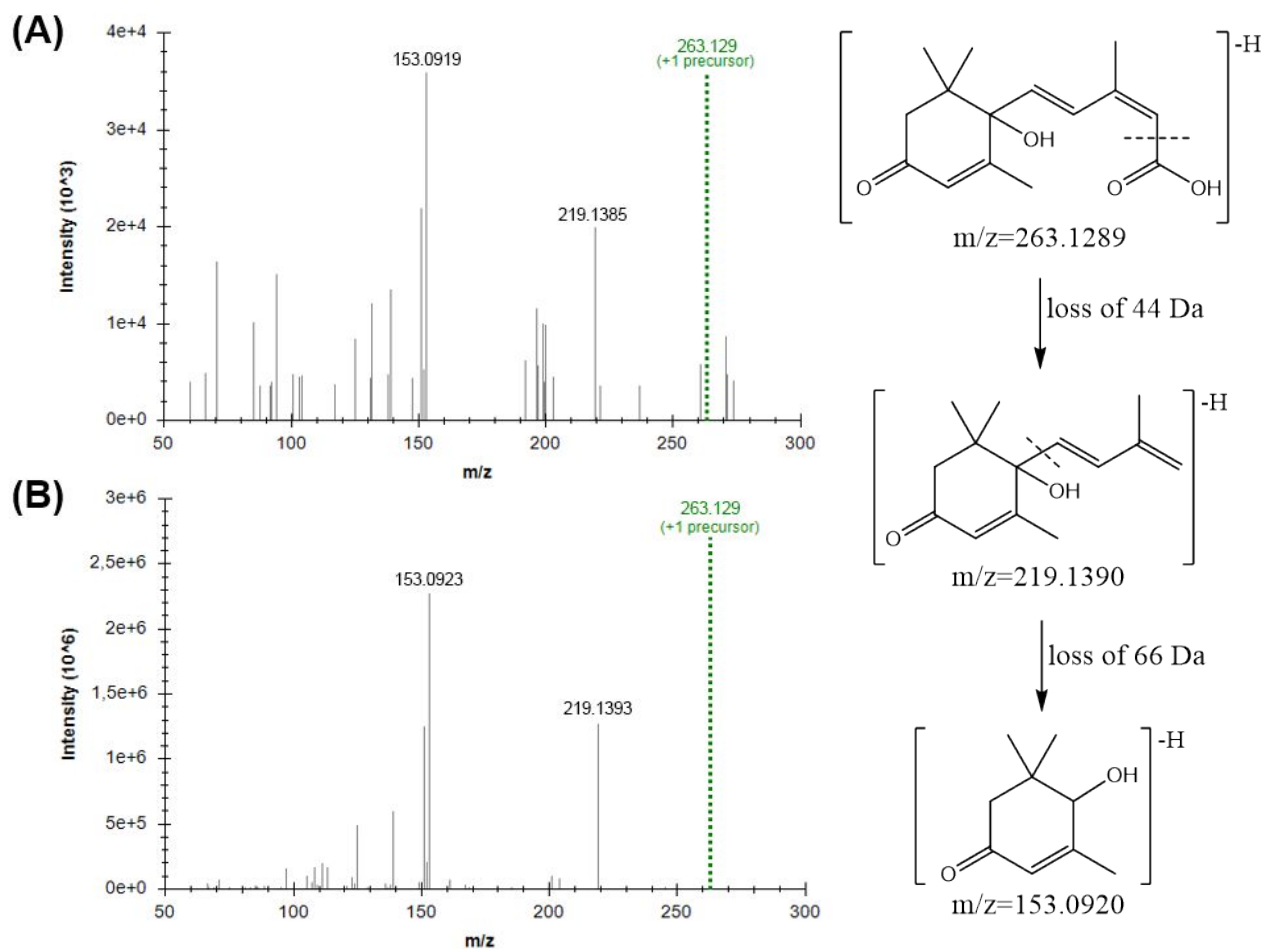


Figure S2 – Comparison of the MS² spectra acquired in negative ionization mode of (A) the product ion (m/z 263.1288) of peak 9 annotated as abscisic acid glucuronide in serum samples and (B) abscisic acid reference standard. The hypothesized scheme of abscisic acid fragmentation explaining the experimental spectra is also shown.

